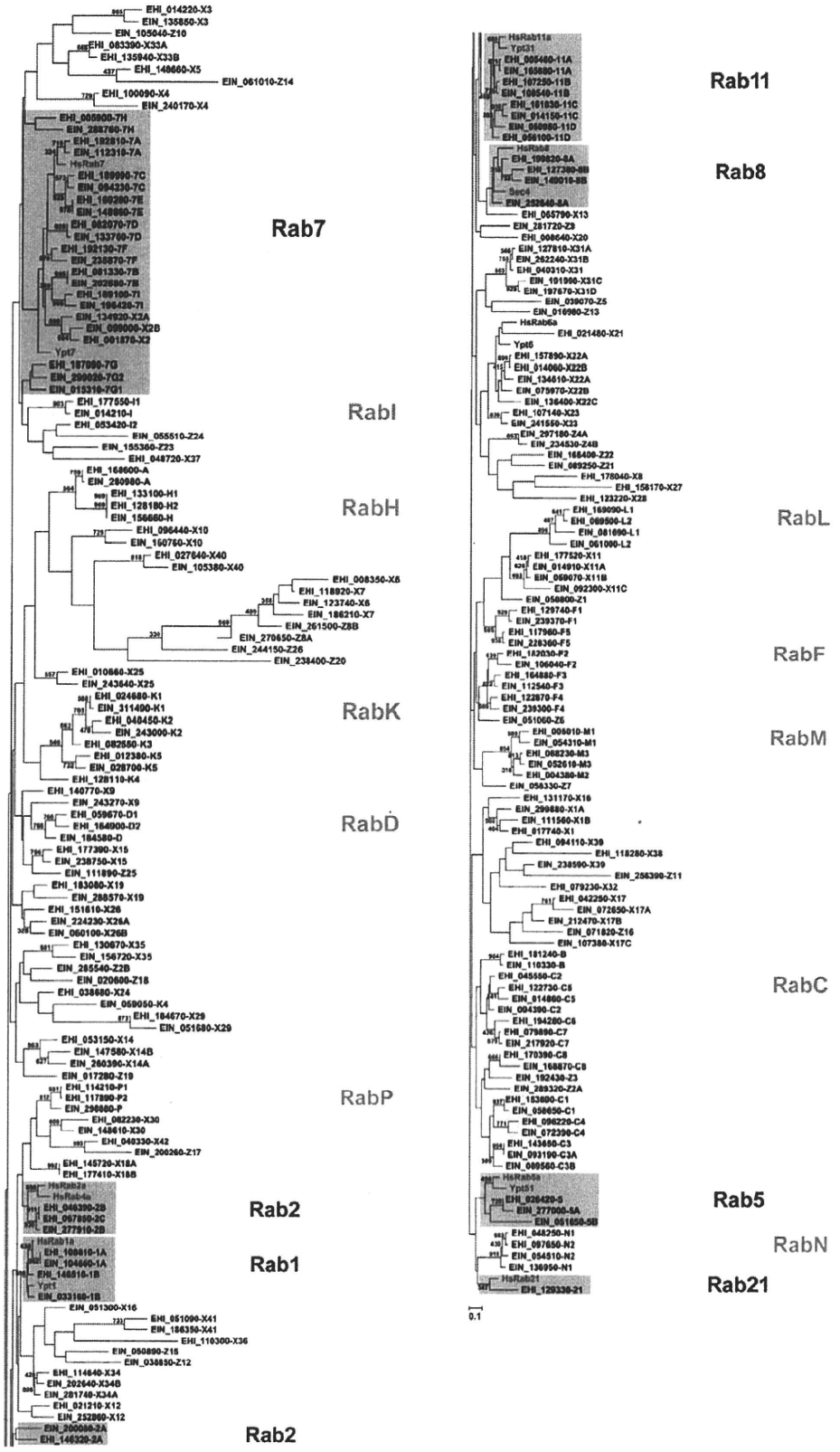

Fig. 1. Phylogenetic analysis of Rab proteins from *E. histolytica*, *E. invadens*, yeast and humans. Phylogenetic analysis of Rab genes from *E. histolytica*, *E. invadens*, yeast, and humans was performed using CLUSTAL W. Trees were drawn using TreeView. The numbers at the nodes represent bootstrap values for 1000 iterations shown in percentages. Yeast and human Rabs are indicated by Ypt and HsRab, respectively. Rabs from *E. histolytica* and *E. invadens* are indicated with their identification number (Table 1; starting with EHI or EIN for *E. histolytica* or *E. invadens* entries, respectively) followed by the subfamily name and number in its abbreviated form. Subfamilies that revealed significant homology (>40% identity) to yeast and human (e.g., Rab5) are shown in dark shaded boxes, while *Entamoeba*-specific subfamilies that contain multiple isotypes are shown in light shaded boxes. The scale bar indicates 0.1 substitutions at each amino acid.

exception of Rab2C. The relative proportion of ubiquitous Rabs conserved in eukaryotes (Rab1~21), *Entamoeba*-specific (i.e., conserved in the two *Entamoeba* species, but not present in other eukaryotes) Rabs (RabA~Z), and species-specific Rabs are similar between *E. histolytica* and *E. invadens* (Fig. 2).

3.1.3. Rabs conserved between E. histolytica and E. invadens

Some Rab subfamilies or isotypes consist of different numbers of isotypes or subisotypes in *E. histolytica* and *E. invadens* (Table 2). Eighty-five percent of Rabs that form subfamilies (e.g., RabC) are conserved (Table 1), suggesting the shared house-keeping roles of these Rab subfamilies in *Entamoeba*. The only exceptions are the RabX18 and RabX33 subfamilies that consist of two isotypes in *E. histolytica*, but are not conserved in *E. invadens*. Conversely, 38% of the solitary (i.e., not forming a subfamily) Rabs are not conserved in *E. invadens*.

3.1.4. Rabs specific to E. histolytica or E. invadens

Among Rab proteins conserved in eukaryotes (Rab1~21), *E. invadens* has additional isotypes of Rab5 and Rab7G, EiRab5B and EiRab7G2, respectively. *E. histolytica* has one each of EhRab5 and EhRab21 that are categorized into the Rab5/Rab21 group (Pereira-Leal and Seabra, 2001). While two EiRab5 isotypes show a 50–83% identity to EhRab5, they show only a 32–33% identity to EhRab21, and were thus annotated as a Rab5 isotype. Phylogenetic analysis (Fig. 1) also supported this annotation.

The number of isotypes and subisotypes in 12 subfamilies and isotypes (Rab5B, 7G2, C3, X1B, X2B, X11B–C, X14B, X17B–C, X22C, X26B, X31B–D, and X34B) is higher in *E. invadens* than in *E. histolytica* (Table 2). In addition, 29 *E. invadens* Rabs (EiRabZ1–26) that show low (<40%) similarity to *E. histolytica* Rabs were discovered and considered to have independently evolved in *E. invadens*. Conversely, homologues corresponding to 26 *E. histolytica* Rabs were not identified in the current *E. invadens* database; however, the lack of these Rabs in *E. invadens* must be confirmed due to the lower coverage of the *E. invadens* genome.

3.2. Review of the demonstrated functions of Rabs in Entamoeba

Although several previous proteomic and transcriptomic studies (see below) suggested that a few dozens of Rab genes/proteins are involved in important biological processes, such as stress response, pathogenesis, and stage conversion, these Rab genes were not discussed. This is partly due to the lack of proper annotation of *Entamoeba* Rab genes at the time of publication. In this section, we summarize the current understanding of the reported functions of Rabs, and also review the previous transcriptomic and proteomic studies that indicate the roles of Rab genes in stress response, pathogenesis, and stage conversion.

Table 2
Rab subfamilies and isotypes that vary in number between *E. histolytica* and *E. invadens*. Seventeen Rab families that have different numbers of isotypes and two isotypes (EhRab7G and EhRabC3) that are encoded by two independent genes are shown.

Rab subfamily/isotype	Number of Rab isotypes	
	E. histolytica	*E. invadens*
Rab2	3	2
Rab5	1	2
Rab7G	1	2
RabC3	1	2
RabD	2	1
RabH	2	1
RabI	2	1
RabK	5	4
RabM	3	2
RabP	2	1
RabX1	1	2
RabX2	1	2
RabX11	1	3
RabX14	1	2
RabX17	1	3
RabX22		3
RabX26	1	2
RabX31	1	4
RabX34	1	2

3.2.1. Demonstrated functions of E. histolytica Rabs

Among all annotated Rabs, there are only a dozen for which their localization, function, or both have been demonstrated. Among the multiple EhRab7 isotypes, EhRab7B is involved in lysosome biogenesis (Fig. 3; Saito-Nakano et al., 2007), while EhRab7A is involved in the targeting of hydrolases to lysosomes (Nakada-Tsukui et al., 2005; Saito-Nakano et al., 2007). EhRab7A, together with EhRab5, also coordinately regulates the formation and matu-

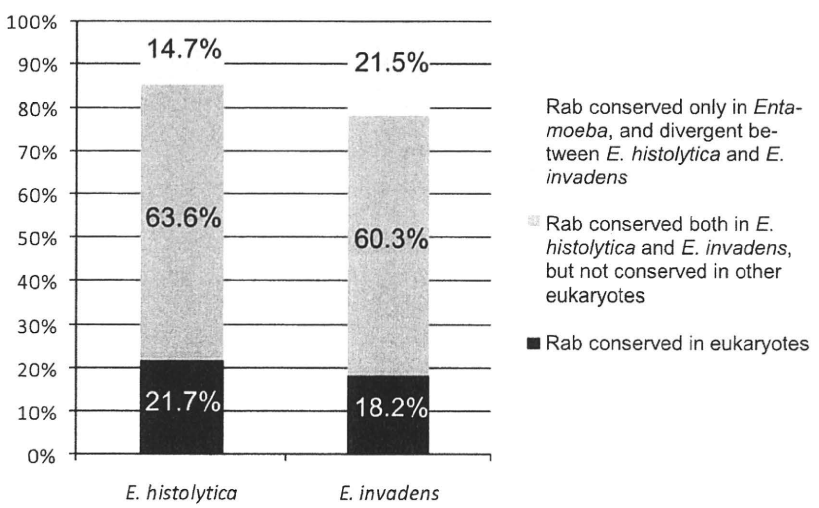

Fig. 2. Percentages of conserved and genus- or species-specific Rab genes in *E. histolytica* and *E. invadens*. Percentage of Rab genes conserved in eukaryotes (Rab1~21, black bars), Rab genes conserved in *E. histolytica* and *E. invadens*, but not conserved in other eukaryotes (RabA~Z, dark shaded bars), and Rab genes conserved only in *Entamoeba* and divergent between *E. histolytica* and *E. invadens* (light shaded bars).

ration of the prephagosomal vacuole (PPV), a unique organelle in *E. histolytica* that is formed during phagocytosis, and is likely to be involved in the processing, activation, or storage of hydrolases that are transported to the phagosome (Saito-Nakano et al., 2004). *E. histolytica*-specific EhRabA was initially suggested to be involved in motility and polarization (Welter et al., 2005), and has been recently shown to be involved in the transport of the Gal/GalNAc-specific lectin (Welter and Temesvari, 2009). EhRab11A was reported to be recruited to the cell surface by iron or serum starvation, and was suggested to be involved in encystation (McGugan and Temesvari, 2003). In contrast, EhRab11B is involved in cysteine protease secretion, and its overexpression enhanced the secretion of cysteine protease (Mitra et al., 2007).

The proteomic analysis of phagosomes isolated from *E. histolytica* trophozoites revealed a panel of phagosome-associated Rabs (Fig. 3; Marion et al., 2005; Okada et al., 2005, 2006). Among the phagosome-associated Rabs, RabD2, P2, and X37 are not conserved in *E. invadens* (Table 1). Interestingly, EhRabD2 and EhRabX37 were expressed only in trophozoites, but not in cysts; their expression was also downregulated during oxidative stress (Table 3, see below). The role of these Rabs appears to be specific to *E. histolytica*, and may be associated with virulence. It needs to be confirmed by proteomic analysis of isolated *E. invadens* phagosomes whether Rab proteins and other phagosome proteins are shared by both species.

3.2.2. Stress- or infection-induced regulation of Rab gene expression

Previous transcriptomic studies indicated that several Rab genes are transcriptionally regulated during stress, stage conversion, and animal infection (Table 3). Incubation of trophozoites at 42 °C for 1 h caused the upregulation of the EhRab7A gene by 2-fold (MacFarlane et al., 2005). It was also shown that the levels

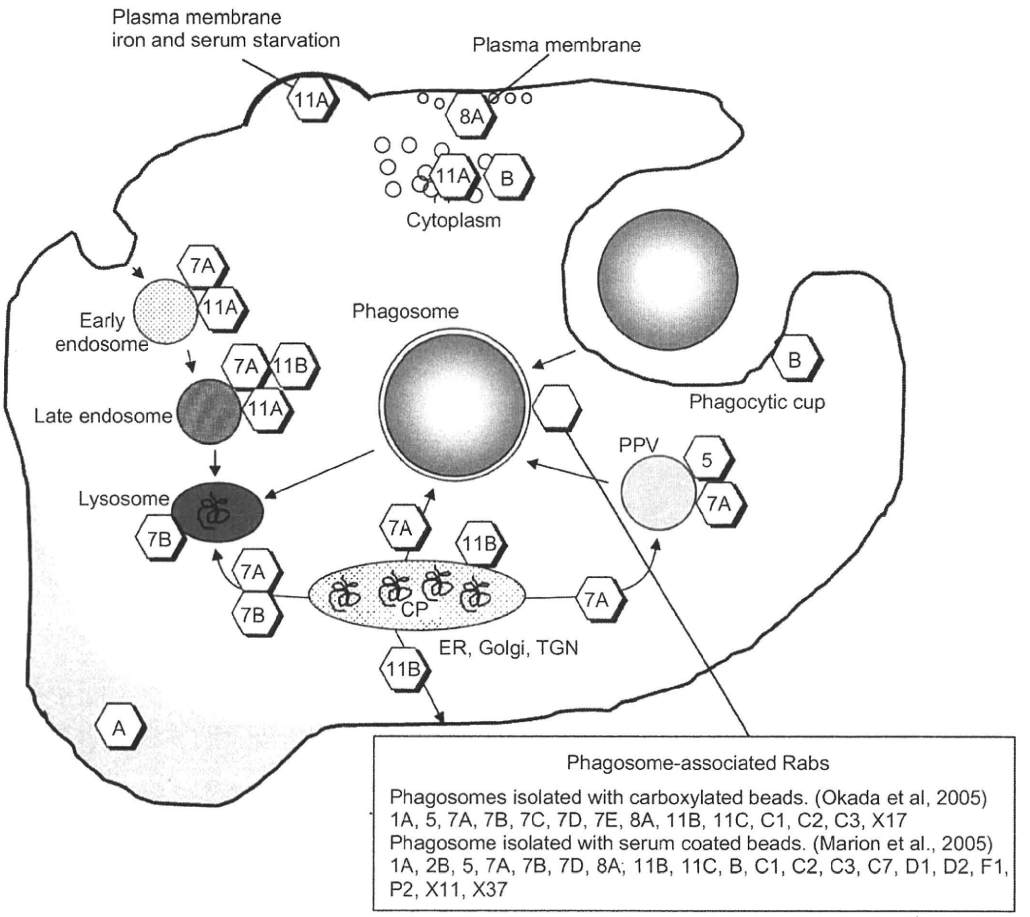

Fig. 3. Demonstrated and presumed localization and function of *E. histolytica* Rabs. Summarized scheme of the localization and function of selected *E. histolytica* Rab proteins is shown based on previous publications. (1) Endosomes: EhRab7A, EhRab11A, and EhRab11B were demonstrated to be localized to endosomes by immunofluorescence assay (EhRab7A and EhRab11B), or immunoblot analysis using iron-dextran-containing endosomes isolated using magnetic separation (EhRab7A and EhRab11A) (Temesvari et al., 1999; Saito-Nakano et al., 2004; Nakada-Tsukui et al., 2005; Mitra et al., 2007). EhRab11A was not demonstrated to be located on endosomes by immunofluorescence, but was suggested to be translocated to the cell surface upon iron and serum starvation or encystation (McGugan and Temesvari, 2003). (2) Phagosomes: EhRabB was localized to the phagocytic cup (Rodriguez et al., 2000). Phagosome-associated Rab proteins, demonstrated by proteomic analysis of isolated phagosomes using carboxylated beads (Okada et al., 2005) or serum-coated beads (Marion et al., 2005), are found in the islet. All Rab proteins detected at various time points of phagocytosis in different strains are listed. (3) Prephagosomal vacuoles (PPV): PPV were reported to be a reservoir of cysteine proteases and other digestive enzymes transported to the phagosome, and EhRab5 and EhRab7A were localized to PPV (Saito-Nakano et al., 2004). (4) Lysosomes: EhRab7A is involved in the transport of cysteine proteases to phagosomes and lysosomes, and a partial association of EhRab7A with lysosomes was observed (Nakada-Tsukui et al., 2005; Saito-Nakano et al., 2007). EhRab11B was suggested to be involved in the transport of cysteine proteases (Mitra et al., 2007), although its exact localization remains unknown. EhRab7B was present in lysosomes and involved in lysosome biogenesis, together with EhRab7A (Saito-Nakano et al., 2007). (5) Secretory vesicles or post-Golgi compartments: EhRab8 showed peripheral dotted localization underneath the plasma membrane, and was suggested to be involved in secretion (Juarez et al., 2001). (6) Unknown compartments in the cytoplasm: EhRabB revealed a punctate dotted localization throughout the cytoplasm, but its exact localization remains to be determined (Rodriguez et al., 2000). EhRabA was localized to the leading edge of the cell and was presumed to regulate cell motility and polarization (Welter and Temesvari, 2004; Welter et al., 2005). Furthermore, the overexpression of dominant negative EhRabA caused an alteration of ER morphology and the localization of the Gal/GalNAc-specific lectin (Welter and Temesvari, 2009).

Table 3
Rab genes that are differentially expressed.

Rab gene	Fold change	Up/down	Condition/stage/strain	Method[a]	Reference[b]
Ehrab5	3.62	Down	Cyst (vs. trophozoite)	D	a
	3.2	Down	*E. dispar* (vs. *E. histolytica*)	D	b
Ehrab7A	2	Up	Heat shock[c]	D	c
Ehrab7D	25.37	Up	Avirulent HM-1 (vs. virulent HM-1)	D	d
	3.55	Down	Cyst (vs. trophozoite)	D	a
Ehrab7E	62	Up	Avirulent HM-1 (vs. virulent HM-1)	D	d
Ehrab7F	4.8	Down	Oxidative stress[e], HM-1	D	e
	4.4	Down	NO stress[f]	D	
Ehrab7G	14.5	Up	Avirulent HM-1 (vs. virulent HM-1)	D	d
Ehrab11A	4.23	Down	Cyst (vs. trophozoite)	D	a
Ehrab11B	4.55	Down	Cyst (vs. trophozoite)	D	a
Ehrab11D	8.43	Down	Cyst (vs. trophozoite)	D	a
EhrabB	5	Up	Heat shock[d]	P	f
	3.32	Down	Cyst (vs. trophozoite)	D	a
EhrabC1	2.2	Down	Cyst (vs. trophozoite)	D	a
EhrabC2	2.2	Down	NO stress[f]	D	e
EhrabC5	3.66	Down	Cyst (vs. trophozoite)	D	a
EhrabC6	6.15	Down	Cyst (vs. trophozoite)	D	a
EhrabD2	5.52	Down	Cyst (vs. trophozoite)	D	a
	2.8	Down	Oxidative stress[e], HM-1	D	e
EhrabH1	3.41	Down	Cyst (vs. trophozoite)	D	a
EhrabI1	3.56	Up	Oxidative stress[e], HM-1	D	e
	3.5	Up	NO stress[f]	D	
EhrabK2	7.14	Down	Cyst (vs. trophozoite)	D	a
EhrabL1	2.7	Down	NO stress[f]	D	e
EhrabM1	6.7	Up	Cyst (vs. trophozoite)	D	a
	2	Up	Oxidative stress[c], HM-1	D	e
EhrabM2	3.65	Down	Cyst (vs. trophozoite)	D	a
EhrabNI	4.1	Up	Cyst (vs. trophozoite)	D	a
EhrabX6	4.76	Down	*E. dispar* (vs. *E. histolytica*)	D	b
EhrabX13	2	Down	*E. dispar* (vs. *E. histolytica*)	D	b
EhrabX14	2.95	Up	Day 1 of intestinal challenge	D	g
	2.86	Up	Day 29 of intestinal challenge	D	
EhrabX15	3	Up	NO stress[f]	D	e
EhrabX19	5.1	Down	NO stress[f]	D	e
EhrabX31	2	Up	Oxidative stress[c], Rhaman	D	e
EhrabX32	2.7	Up	NO stress[f]	D	e
EhrabX35	2.3	Up	Oxidative stress[e], Rhaman	D	e
	2	Up	NO stress[f]	D	
EhrabX37	3.84	Down	Cyst (vs. trophozoite)	D	a
EhrabX42	2.43	Down	NO stress[f]	D	e

[a]D, DNA microarray; P, real-time PCR.
[b](a) Ehrenkaufer et al. (2007), (b) MacFarlane and Singh (2006), (c) MacFarlane et al. (2005), (d) Biller et al. (2010), (e) Vicente et al. (2009), (f) Romero-Diaz et al. (2007), (g) Gilchrist et al. (2006).
[c]42 °C, 1 h.
[d]42 °C, 5 h.
[e]1 mM H_2O_2, 1 h.
[f]HM-1, 200 μM dipropylenetriamine (DPTA)-NONNate, 1 h.

of the EhRabB transcript increased by 5-fold after incubation at 42 °C for 5 h (Romero-Diaz et al., 2007). It was suggested that the putative heat shock elements (HSE) upstream of the EhRabB gene are involved in the regulation of EhRabB (Romero-Diaz et al., 2007). It was also shown that incubation of trophozoites from the HM-1 and Rhaman strains with hydrogen peroxide or the nitric oxide donor dipropylenetriamine-NONOate (DPTA), caused a 4-fold upregulation of EhRabI1, and a 4.4–4.8-fold downregulation of EhRab7F (Vicente et al., 2009). Since these Rabs appeared to be regulated in a similar way by hydrogen peroxide and nitric oxide, common regulator(s) and pathway(s) may be involved in the responses against these stresses. It should be noted that some Rab genes differentially respond to oxidative and nitric oxide stress. For example, EhRabM1 and EhRabX31 were upregulated only by hydrogen peroxide, while EhRabX15, X32, and X35 were upregulated only by DPTA (Vicente et al., 2009). Similarly, EhRabD2 was downregulated by oxidative stress, whereas EhRabC2, L1, and X19 were downregulated by nitric oxide (Vicente et al., 2009). Although the role of these Rabs remains unknown, these findings indicate a possible link between oxidative/nitrosative stress response and membrane trafficking. In addition, it was shown that during mouse intestinal infection, EhRabX14 expression was upregulated on days 1 and 29 post-infection (Gilchrist et al., 2006). These change in expression may also be a consequence of the stress response because amoebae are exposed to reactive oxygen and nitrogen species during host invasion.

3.2.3. Differences in Rab gene expression between E. histolytica and E. dispar, and between virulent and avirulent E. histolytica strains

A comparison of the transcriptome of the non-pathogenic sibling *E. dispar* and *E. histolytica* also revealed that Rab5, X6, and X13 were downregulated in *E. dispar* (MacFarlane and Singh, 2006). Since Rab5 plays a role in the formation of the PPV in *E. histolytica* (Saito-Nakano et al., 2004), the repression of Rab5 expression in *E. dispar* may indicate the suppressed activity of phagocytosis and endocytosis in *E. dispar* (Mitra et al., 2005). Recently, transcriptomic analysis of two HM-1 strains with different abilities to form amoebic liver abscess was reported (Biller et al., 2010). The expression of three Rab7 subfamilies, EhRab7D, 7E, and 7G, was augmented in the avirulent HM-1 strain, obtained

from American Type Culture Collection (ATCC). In contrast, EhRab7D and 7G were poorly transcribed in an independently established attenuated HM-1 strain (Mitra et al., 2006; Saito-Nakano et al., 2007). These data suggest that the expression of individual Rab7 isotypes may be largely affected by subtle changes in the *in vitro* culture conditions.

3.2.4. Regulation of Rab gene expression during stage conversion

Several EhRab genes have been suggested to play a role in the stage conversion of *E. histolytica* (Ehrenkaufer et al., 2007). Transcriptomic analysis of clinical isolates and an attenuated HM-1 strain showed that EhRabM1 and EhRabN1 were expressed 6.7- and 4.1-fold higher in clinical isolates, respectively, than in HM-1 (Table 3). Since the clinical isolates used partially retained an ability to encyst *in vitro*, which attenuated HM-1 strain had lost, these data may indicate that the aforementioned Rabs are likely to be upregulated in the cyst or during encystation. In contrast, Rab5, 7D, 11A, 11B, 11D, B, C1, C5, C6, D2, H1, K2, M2, and X37, were expressed at higher levels in the laboratory strain, which does not encyst, compared to the clinical isolates, suggesting that these Rabs may be upregulated in the trophozoite stage (Ehrenkaufer et al., 2007). EhRabM1 was upregulated in the cyst stage and by oxidative stress, which may suggest a common role of EhRabM1 in stress response and differentiation. It is worth examining whether these changes are found in the cyst-like form of *E. histolytica* induced by oxidative stress (Aguliar-Diaz et al., 2010).

In summary, we proposed the annotation of *E. invadens* and *E. histolytica* Rab genes. Comparison of the Rab repertoire between the two species demonstrated that the majority of Rabs is conserved between the two species, while there are also species-specific Rabs. To understand the individual roles of Rabs, further functional studies are necessary. For instance, comprehensive transcriptomic analysis of Rab genes during the encystation of *E. invadens* should identify stage-specific regulated Rab genes and reveal ubiquitous or species-specific Rab-mediated encystation mechanisms in *Entamoeba*.

Acknowledgments

We thank Lis Caler, Bioinformatics Resource Center, J. Craig Venter Institute for sharing unpublished information of the *E. invadens* genome, and Takashi Makiuchi for his help with the phylogenetic analyses. We thank Eiko Nakasone for her help in the search for Rab genes from *E. invadens*. This work was supported by Creative Scientific Research (18GS0314) from the Japanese Ministry of Education, Science, Culture, Sports, and Technology to T.N., a Grant-in-Aid for Scientific Research from the Japanese Ministry of Education, Culture, Sports, Science, and Technology to T.N. (18GS0314, 18050006, and 18073001), a grant for research on emerging and re-emerging infectious diseases from the Japanese Ministry of Health, Labour, and Welfare, and a grant for research to promote the development of anti-AIDS pharmaceuticals from the Japan Health Sciences Foundation to T.N.

References

Aguliar-Diaz, H., Diaz-Gallardo, M., Laclette, J.P., Carrero, C.J., 2010. In vitro induction of *Entamoeba histolytica* cyst-like structures from trophozoites. PLoS Neglected Tropical Diseases 4, e607.

Biller, L., Davis, P.H., Tillack, M., Matthiesen, J., Lotter, H., Stanley, S.L., Tannich, E., Bruchhaus, I., 2010. Differences in the transcriptome signatures of two genetically related *Entamoeba histolytica* cell lines derived from the same isolate with different pathogenic properties. BMC Genomics 11, 63.

Bourne, H.R., Sanders, D.A., McCormick, F., 1990. The GTPase superfamily: a conserved switch for diverse cell functions. Nature 348, 125–132.

Carlton, J.M., Hirt, R.P., Silva, J.C., Delcher, A.L., Schantz, M., Zhao, Q., Wortman, J.R., Bidwell, S.L., Alsmark, U.C., Besterio, S., Sicheritz-Ponten, T., Noel, C.J., Dacks, J.B., Foster, P.G., Simillion, C., et al., 2007. Draft genome sequence of the sexually transmitted pathogen *Trichomonas vaginalis*. Science 315, 207–212.

Chatterjee, A., Ghosh, S.K., Jang, K., Bullitt, E., Moore, L., Robbins, P.W., Samuelson, J., 2009. Evidence for a "wattle and daub" model of the cyst wall of *Entamoeba*. PLoS Pathogens 5, e1000498.

Ehrenkaufer, G.M., Haque, R., Hackney, J.A., Eichinger, D.J., Singh, U., 2007. Identification of developmentally regulated genes in *Entamoeba histolytica*: insights into mechanisms of stage conversion in a protozoan parasite. Cellular Microbiology 9, 1426–1444.

Eichinger, D., 1997. Encystation of *Entamoeba* parasites. Bioessays 19, 633–639.

Eichinger, D., 2001. Encystation in parasitic protozoa. Current Opinion in Microbiology 4, 421–426.

Gilchrist, C.A., Houpt, E., Trapaidze, N., Fei, Z., Crasta, O., Asgharpour, A., Evans, C., Martino-Catt, S., Baba, D.J., Stroup, S., Hamano, S., Ehrenkaufer, G., Okada, M., Singh, U., Nozaki, T., Mann, B.J., Petri Jr., W.A., 2006. Impact of intestinal colonization and invasion on the *Entamoeba histolytica* transcriptome. Molecular and Biochemical Parasitology 147, 163–176.

Juarez, P., Sanchez-Lopez, R., Stock, R.P., Olvera, A., Ramos, M.A., Alagon, A., 2001. Characterization of the EhRab8 gene, a marker of the late stages of the secretory pathway of *Entamoeba histolytica*. Molecular and Biochemical Parasitology 116, 223–228.

MacFarlane, R.C., Singh, U., 2006. Identification of differentially expressed genes in virulent and nonvirulent *Entamoeba* species: potential implications for amebic pathogenesis. Infection and Immunity 74, 340–351.

MacFarlane, R., Bhattacharya, D., Singh, U., 2005. Genomic DNA microarrays for *Entamoeba histolytica*: applications for use in expression profiling and strain genotyping. Experimental Parasitology 110, 196–202.

Marion, S., Laurent, C., Guillén, N., 2005. Signalization and cytoskeleton activity through myosin IB during the early steps of phagocytosis in *Entamoeba histolytica*: a proteomic approach. Cellular Microbiology 7, 1504–1518.

McGugan Jr., G.C., Temesvari, L.A., 2003. Characterization of a Rab11-like GTPase, EhRab11, of *Entamoeba histolytica*. Molecular and Biochemical Parasitology 129, 137–146.

Mitra, B.N., Yasuda, T., Kobayashi, S., Saito-Nakano, Y., Nozaki, T., 2005. Differences in morphology of phagosomes and kinetics of acidification and degradation in phagosomes between the pathogenic *Entamoeba histolytica* and the non-pathogenic *Entamoeba dispar*. Cell Motility and Cytoskeleton 62, 84–99.

Mitra, B.N., Kobayashi, S., Saito-Nakano, Y., Nozaki, T., 2006. *Entamoeba histolytica*: differences in phagosome acidification and degradation between attenuated and virulent strains. Experimental Parasitology 114, 57–61.

Mitra, B.N., Saito-Nakano, Y., Nakada-Tsukui, K., Sato, D., Nozaki, T., 2007. Rab11B small GTPase regulates secretion of cysteine proteases in the enteric protozoan parasite *Entamoeba histolytica*. Cellular Microbiology 9, 2112–2125.

Nakada-Tsukui, K., Saito-Nakano, Y., Ali, V., Nozaki, T., 2005. A retromerlike complex is a novel Rab7 effector that is involved in the transport of the virulence factor cysteine protease in the enteric protozoan parasite *Entamoeba histolytica*. Molecular Biology of the Cell 16, 5294–5303.

Novick, P., Zerial, M., 1997. The diversity of Rab proteins in vesicle transport. Current Opinion in Cell Biology 9, 496–504.

Nozaki, T., Nakada-Tsukui, K., 2006. Membrane trafficking as a virulence mechanism of the enteric protozoan parasite *Entamoeba histolytica*. Parasitology Research 98, 179–183.

Okada, M., Huston, C.D., Mann, B.J., Petri Jr., W.A., Kita, K., Nozaki, T., 2005. Proteomic analysis of phagocytosis in the enteric protozoan parasite *Entamoeba histolytica*. Eukaryotic Cell 4, 827–831.

Okada, M., Huston, C.D., Oue, M., Mann, B.J., Petri Jr., W.A., Kita, K., Nozaki, T., 2006. Kinetics and strain variation of phagosome proteins of *Entamoeba histolytica* by proteomic analysis. Molecular and Biochemical Parasitology 145, 171–183.

Pereira-Leal, J.B., Seabra, M.C., 2000. The mammalian Rab family of small GTPases: definition of family and subfamily sequence motifs suggests a mechanism for functional specificity in the Ras superfamily. Journal of Molecular Biology 301, 1077–1087.

Pereira-Leal, J.B., Seabra, M.C., 2001. Evolution of the Rab family of small GTP-binding proteins. Journal of Molecular Biology 313, 889–901.

Picazarri, K., Nakada-Tsukui, K., Nozaki, T., 2008. Autophagy during proliferation and encystation in the protozoan parasite *Entamoeba invadens*. Infection and Immunity 76, 278–288.

Rodriguez, M.A., Garcia-Perez, R.M., Garcia-Rivera, G., Lopez-Reyes, I., Mendoza, L., Ortiz-Navarrete, V., Orozco, E., 2000. An *Entamoeba histolytica* rab-like encoding gene and protein: function and cellular location. Molecular and Biochemical Parasitology 108, 199–206.

Romero-Diaz, M., Gomez, C., Lopez-Reyes, I., Martinez, M.B., Orozco, E., Rodriguez, M.A., 2007. Structural and functional analysis of the *Entamoeba histolytica* EhrabB gene promoter. BMC Molecular Biology 8, 82.

Saito-Nakano, Y., Yasuda, T., Nakada-Tsukui, K., Leippe, M., Nozaki, T., 2004. Rab5-associated vacuoles play a unique role in phagocytosis of the enteric protozoan parasite *Entamoeba histolytica*. Journal of Biological Chemistry 279, 49497–49507.

Saito-Nakano, Y., Loftus, B.J., Hall, N., Nozaki, T., 2005. The diversity of Rab GTPases in *Entamoeba histolytica*. Experimental Parasitology 110, 244–252.

Saito-Nakano, Y., Mitra, B.N., Nakada-Tsukui, K., Sato, D., Nozaki, T., 2007. Two Rab7 isotypes, EhRab7A and EhRab7B, play distinct roles in biogenesis of lysosomes and phagosomes in the enteric protozoan parasite *Entamoeba histolytica*. Cellular Microbiology 9, 1796–1808.

Saitou, N., Nei, M., 1987. The neighbor-joining method: a new method for reconstructing phylogenetic trees. Molecular Biology of Evolution 4, 406–425.

Singh, U., Ehrenkaufer, G.M., 2009. Recent insights into *Entamoeba* development: identification of transcriptional networks associated with stage conversion. International Journal of Parasitology 39, 41–47.

Stenmark, H., 2009. Rab GTPases as coordinators of vesicle traffic. Nature Reviews Molecular Cell Biology 10, 513–525.

Takai, Y., Sasaki, T., Matozaki, T., 2001. Small GTP-binding proteins. Physiological Reviews 81, 153–208.

Temesvari, L.A., Harris, E.N., Stanely, S.L., Cardelli, J.A., 1999. Early and late endosomal compartments of *Entamoeba histolytica* are enriched in cysteine proteases, acid phosphatase and several Ras-related Rab GTPases. Molecular and Biochemical Parasitology 103, 225–241.

Thompson, D.J., Higgins, D.G., Gibson, T.J., 1994. CLUSTAL W: improving the sensitivity of program multiple sequence alignment through sequence weighting, positive-specific gap penalties and weight matrix choice. Nucleic Acids Research 22, 4673–4680.

Vicente, J.B., Ehrenkaufer, G.M., Saraiva, L.M., Teixeira, M., Singh, U., 2009. *Entamoeba histolytica* modulates a complex repertoire of novel genes in response to oxidative and nitrosative stresses: implications for amebic pathogenesis. Cellular Microbiology 11, 51–69.

Wang, Z., Samuelson, J., Clark, C.G., Eichinger, D., Paul, J., Van Dellen, K., Hall, N., Anderson, I., Loftus, B., 2003. Gene discovery in the *Entamoeba invadens* genome. Molecular and Biochemical Parasitology 129, 23–31.

Welter, B.H., Temesvari, L.A., 2004. A unique Rab GTPase, EhRabA, of *Entamoeba histolytica*, localizes to the leading edge of motile cells. Molecular and Biochemical Parasitology 135, 185–195.

Welter, B.H., Temesvari, L.A., 2009. Overexpression of a mutant form of EhRabA, a unique Rab GTPase of *Entamoeba histolytica*, alters endoplasmic reticulum morphology and localization of the Gal/GalNAc adherence lectin. Eukaryotic Cell 8, 1014–1026.

Welter, B.H., Powell, R.R., Leo, M., Smith, C.M., Temesvari, L.A., 2005. A unique Rab GTPase, EhRabA, is involved in motility and polarization of *Entamoeba histolytica* cells. Molecular and Biochemical Parasitology 140, 161–173.

Parasitology International 60 (2011) 75–83

Contents lists available at ScienceDirect

Parasitology International

journal homepage: www.elsevier.com/locate/parint

Transcripts analysis of infective larvae of an intestinal nematode, *Strongyloides venezuelensis*

Ayako Yoshida [a], Eiji Nagayasu [a], Anna Nishimaki [a], Akira Sawaguchi [b], Sayaka Yanagawa [a], Haruhiko Maruyama [a,*]

[a] Department of Infectious Diseases, Division of Parasitology, Faculty of Medicine, University of Miyazaki, Miyazaki, Japan
[b] Department of Anatomy, Division of Ultrastructural Cell Biology, Faculty of Medicine, University of Miyazaki, Miyazaki, Japan

ARTICLE INFO

Article history:
Received 14 April 2010
Received in revised form 4 October 2010
Accepted 27 October 2010
Available online 5 November 2010

Keywords:
Strongyloides
Nematode
Infective larva
EST

ABSTRACT

Free-living infective larvae of *Strongyloides* nematodes fulfill a number of requirements for the successful infection. They need to endure a long wait in harsh environmental conditions, like temperature, salinity, and pH, which might change drastically from time to time. Infective larvae also have to deal with pathogens and potentially hazardous free-living microbes in the environment. In addition, infective larvae must recognize the adequate host properly, and start skin penetration as quickly as possible. All these tasks are essentially important for the survival of *Strongyloides* nematodes, however, our knowledge is extremely limited in any one of these aspects. In order to understand how *Strongyloides* infective larvae meet these requirements, we examined transcripts of infective larvae by randomly sequencing cDNA clones constructed from *S. venezuelensis* infective larvae. After assembling successfully sequenced clones, we obtained 162 unique singletons and contigs, of which 84 had been significantly annotated. Annotated genes included those for respiratory enzymes, heat-shock proteins, neuromuscular proteins, proteases, and immunodominant antigens. Genes for lipase, small heat-shock protein, globin-like protein and cytochrome *c* oxidase were most abundantly transcribed, though genes of unknown functions were also abundantly transcribed. There were no hits found against NCBI or NEMABASE4 for 37 (22.3%) EST out of the total 162 EST. Although most of the transcripts were not infective larva-specific, the expression of respiration related proteins was most actively transcribed in the infective larva stage. The expression of astacin-like metalloprotease, small heat-shock protein, *S. stercoralis* L3Nie antigen homologue, and one unannotated and 2 novel genes was highly specific for the infective larva stage.

1. Introduction

Strongyloidiasis is endemic in tropical and subtropical regions, such as Southeast Asia, Latin-America, and sub-Saharan Africa, and endemic foci are present in temperate countries as well, e.g. Mediterranean coast of Spain, southern United States, and Satsunann-Ryukyu Islands in Japan [1–3]. Hundreds of millions of people have been possibly affected globally, though no precise estimate is available.

The key for the control of strongyloidiasis is in the infective larva because the infection starts with this stage of the worm. Free-living infective larvae develop from eggs deposited by free-living females in the soil or parasitic females in the infected host. Infective larvae then wait a host to be infected for some time in the external environment. Considering the life of infective larvae, they obviously face a number of hard tasks before they finally find the host.

First, they are required to endure physical and chemical conditions among them. Temperature, salinity, and pH might change drastically during the wait and chemical compounds could contaminate their surroundings. Second, they have to get rid of or get along with pathogens and potentially hazardous free-living microbes. Among them are various kinds of viruses, bacteria, parasites, and fungi. Infective larvae should be equipped with a kind of defense mechanisms as free-living nematodes are [4,5]. Otherwise they would be heavily infected before they infect the host. In addition to the protection against a number of environmental factors, they must recognize appropriate host animals and start skin penetration as quickly as possible. Failure in host-finding and infection processes would result in the extinction of the species.

Strongyloides infective larvae definitely have solutions to all of the problems and situations described above, however, little is known about their survival and infection strategies [6]. It would be of great scientific and practical significance to understand the biological processes taking place in *Strongyloides* infective larvae. For example, because infection control cannot be done solely with a mass treatment of humans and animals due to the adverse side effects of drugs on biological diversity, new strategies to control the infection have to be explored based on the biology of the nematodes [7,8].

* Corresponding author. 5200 Kihara, Kiyotake, Miyazaki 889-1692, Japan. Tel.: +81 985 85 0990; fax: +81 985 84 3887.
E-mail address: hikomaru@med.miyazaki-u.ac.jp (H. Maruyama).

1383-5769/$ – see front matter © 2010 Elsevier Ireland Ltd. All rights reserved.
doi:10.1016/j.parint.2010.10.007

In the present study, we examined the transcripts of infective larvae by randomly sequencing cDNA clones to clarify the biological processes activated in *S. venezuelensis* infective larvae. We found that the transcripts for respiratory enzymes, heat-shock proteins, neuromuscular proteins, proteases for infection, and an autophagy-related protein were observed. In addition, infective larvae of *S. venezuelensis* abundantly expressed genes which cannot be found in nucleotide databases with significant match. Further analysis of these molecules of unknown functions would greatly facilitate our understanding of the survival strategy of *Strongyloides* nematodes.

2. Materials and methods

2.1. Parasites and animals

Strongyloides venezuelensis has been maintained in male Wistar rats in the Division of Parasitology, Department of Infectious Diseases, University of Miyazaki [9]. ICR mice and Wistar rats were purchased from Kyudo (Kumamoto, Japan). All animals were kept and handled under the approval of the Animal Experiment Committee, University of Miyazaki. The third-stage infective larvae (L3i) were obtained from faecal culture by the filter paper method [10]. L3i were used right after they emerged from the feces (2–3 days after starting faecal culture). Parasitic adult female worms were collected from infected rats 8–10 days post infection (p.i.) [11].

Preparation of larvae in different developmental stages was carried out as previously described [12]. Lung-stage larvae (LL3) were collected as follows; male ICR mice were subcutaneously inoculated with 30,000 L3i, and lungs were removed 72–75 h p.i., homogenized with a Polytron PT-MR3000 (Kinematica AG, Littau, Switzerland) at 20,000 rpm for a few seconds. Lung homogenates were wrapped with Kimwipe papers and incubated in phosphate-buffered saline (PBS) at 37 °C for 1.5 h and emerging worms were collected. Since *S. venezuelensis* has been reported to molt twice in the intestinal mucosa, we designated lung larvae as LL3 [13]. For the preparation of tissue-migrating larvae (L3tm), L3i were injected into the peritoneal cavity of ICR mice, and recovered 20 h p.i. from the peritoneal cavity.

Collected worms were washed with sterile distilled water or PBS extensively, pelleted at the bottom of 2 ml centrifuge tubes then stored at −80 °C until used for RNA preparation (see below).

2.2. cDNA library construction

Infective larvae were homogenized in TRIzol reagent (Invitrogen, Carlsbad, CA, USA) with glass beads for 1.5–2.5 min by a Mini-BeadBeater (Bio Spec Products, Bartlesville, OK, USA), followed by total RNA purification according to the manufacturer's instruction. After treatment with DNaseI (Promega, Madison, WI), poly $(A)^+$ RNA was purified with GenElute mRNA Miniprep Kit (Sigma, Saint Louis, MO).

A cDNA library was constructed using a SMART cDNA library construction kit (Clontech, Mountain View, CA). Reverse transcription (RT) of purified poly $(A)^+$ RNA was performed using MMLV reverse transcriptase with the SMART IV oligonucleotide primer and the CDS III/3′ PCR primer provided in the kit. Double-stranded cDNA (ds-cDNA) was synthesized by long distance PCR with the 5′ PCR primer and the CDS III/3′ PCR primer using the Advantage 2 PCR kit (Clontech). The ds-cDNA was treated with proteinase K and then digested with *Sfi*I. After size fractionation, cDNA was ligated to *Sfi*I-digested pDNR-LIB. The ligation product was then transformed into *Escherichia coli* ElectroMAX DH10B electrocompetent cells (Invitrogen).

2.3. DNA sequencing

Clones were transferred to LB agar plates containing 50 μg/ml chloramphenicol and grown for 20 h prior to colony direct PCR. Insert DNA was amplified from 500 randomly selected clones with a M13 primer set, and PCR products were purified with Post-Reaction Purification Columns (Sigma). Single-pass sequencing was performed from the 5′-end only using M13 forward primer (5′-GTAAAAC-GACGGCCAGT-3′) in ABI PRISM 3130×l Genetic Analyzer (Applied Biosystems, Carlsbad, CA), using ABI PRISM Big-Dye Terminator v3.1 Cycle sequencing kit (Applied Biosystems, Foster City, CA, USA).

2.4. EST processing, contig assembly and analysis

All ESTs were edited out flanking vector and adaptor sequences. After removing rRNA sequences, high quality ESTs longer than 250 bp (408 sequences) were assembled into clusters of contiguous sequences by using Sequencher software (Gene Codes, Ann Arbor, MI, USA). Reads with more than 99% identity were assembled into the same contig. The consensus sequences of contigs and singletons

Table 1
Primer sequences for real-time PCR.

NCBI accession	Associated annotation	Forward primer (5′→3′)	Reverse primer (5′→3′)	Expected product size
HO652180	FMRFamide-related peptide	CATTCACCATCCGAGGTTACTT	GCAAGGGCTTGTTGTAGGG	115
HO652210	Cytochrome P450	GGGAAAAAGAATATGTGCAGGA	TGATAACACCAGAATCGGATGA	132
HO652258	NADH dehydrogenase subunit 6	TGTTGGTTGTTTTGCCAGTT	CCATAACCACAAAAATTCCACTT	99
HO652261	Poly(A)-binding protein	GGTGTCAATGCAGGACAAGTTA	TTGGATAATTCTGTGGGTTTCC	94
HO652553	Hsp90	CCAAGAGGATGCTGGTGATT	TCGAGACAATGCCGACTGTA	84
HO652574	L3Nie Ag (SvL3Nie-2)	GAACCAGAAAAATAAATTGGGAGA	ACTTCATCGTACCAACCTTTTACTCC	87
HO652576	Astacin-like metalloproteinase	GGTGTTGTTACACCCCAAGC	AACAACAATATATTAGTGCAATCGTT	145
HP429054	Globin-like protein	TCCGGAAATGGCAGATTATT	AGGCGGAAGAAACACTGAAA	111
HP429055	Novel[a] (SVC L3ist-1)	TAACCTAAATACTATCTTTTACAATTCC	CAATTCAGTTAATTTCCCTCCA	89
HP429056	Novel[a] (SVC L3ist-2)	TGGAGAGAAATTAACTGAATTGTTGG	TTTTCAATGTTTTTATGCAGGTTC	114
HP429057	*S. stercoralis* Hsp20 (SvHsp-Ss2)	TGGGATTGGCCTTTAAGTCA	GCAGTGAATGTCAATTTTGTCC	147
HP429058	*None*[b] *(PTC 00570_1)*	CGTAGAGGATCCACTGGACA	CATTGATACCAGTATCCATTACAGAGG	85
HP429059	*A. suum* Hsp20 (SvHsp20-As1)	TTTCCTTCCGCCATTCCTAT	TTGAAACGCCCTCATCTCTAA	108
HP429060	Lipase, class 2	TGCAAGTGTGGTAAAGATTGCACATGT	CCTCACAACATTTTGATTCAGCACAGC	88
HP429062	Cytochrome *c* oxidase subunit I	TGCTGGTGGTAATCCTTTGA	ATCCCAAGGGTTCCAAAAAC	151
HP429068	L3Nie Ag (SvL3Nie-1)	CTTGCAGCAAAAGCACAAAA	CAATGGTGAACCAAATGCAA	117
HP429073	*None*[c] *(FC810578.1)*	TGGCCATGGTATGTAGCAAT	ACCCCTAAATGATAGAATGCAGTTGA	131
HP429091	*S. stercoralis* Hsp20 (SvHsp-Ss1)	TTGTGATTGGCCACTTAATGTA	CCTGAATATCCTGTGGGTCAA	113
AB453330.1	18S rebosomal RNA	CCAGCTTTCCAAGTGCATAA	CATCCAAGATGCTCATTACACA	86

[a] Novel; No hits were found in major databases.
[b] Hits were found in NEMABASE4 with no associated annotation.
[c] No hit in NEMABASE4. Match was found in NCBI EST database.

Table 2
S. venezuelensis L3 ESTs with significant annotation by homology search against NEMABASE4.

S. venezuelensis (singleton/contig)		Top hit in Nembase4 (tblastx)				
NCBI accession	Length (bp)	Identifier	Organism	Clade	E-value	Associated annotation
HO652177	601	SSC02297_1	*S. stercoralis*	IV	4.00E−87	Proteasome, subunit alpha/beta
HO652179	576	CRC00223_1	*C. remanei*	V	5.00E−11	RNA recognition motif, RNP-1
HO652180	585	SSC04545_1	*S. stercoralis*	IV	6.00E−45	FMRFamide-related peptide
HO652192	348	SSC00140_1	*S. stercoralis*	IV	3.00E−27	FMRFamide-related peptide
HO652206	292	ACC15350_1	*A. caninum*	V	7.00E−19	Ammonium transporter
HO652209	759	HBC05087_1	*H. bacteriophora*	V	3.00E−83	Cytochrome b/b6
HO652210	406	SRC01426_1	*S. ratti*	IV	4.00E−51	Cytochrome P450
HO652222	427	SSC01666_1	*S. stercoralis*	IV	1.00E−48	Hydroxytetrahydrobiopterindehydratase
HO652225	342	CJC00147_1	*C. japonica*	V	3.00E−15	Signal recognition particle, SRP9 subunit
HO652234	761	SRC00984_2	*S. ratti*	IV	1.00E−153	Ras small GTPase, Ras type
HO652237	564	SSC03440_1	*S. stercoralis*	IV	3.00E−48	LUC7 related
HO652242	636	MJC01056_1	*M. javanica*	IV	2.00E−17	DNA repair protein (XPGC)/yeast Rad
HO652258	389	CSC00005_1	*Caenorhabditis sp.*	V	1.00E−09	NAD Hdehydrogenase (ubiquinone)
HO652261	713	SRC00248_1	*S. ratti*	IV	1.00E−128	Poly(A)-binding protein
HO652283	707	SRC07549_1	*S. ratti*	IV	1.00E−108	Calcium-binding EF-hand
HO652285	867	XIC01943_1	*X. index*	I	2.00E−89	beta-1,4-mannosyltransferase activity
HO652301	574	SRC00826_1	*S. ratti*	IV	7.00E−38	Histone H1/H5
HO652303	620	PTC01840_1	*P. trichosuri*	IV	4.00E−88	NIF system FeS cluster assembly, NifU, N-terminal
HO652319	687	SRC01269_1	*S. ratti*	IV	1.00E−111	Neural proliferation differentiation control-1
HO652339	828	SSC00792_1	*S. stercoralis*	IV	1.00E−103	Klarsicht/ANC-1/syne-1 homology
HO652341	817	LSC00488_1	*L. sigmodontis*	III	4.00E−90	Neurotransmitter-gated ion-channel
HO652363	569	PTC00864_1	*P. trichosuri*	IV	2.00E−99	Isocitrate lyase and phosphorylmutase
HO652371	689	AYC01701_1	*A. ceylanicum*	V	1.00E−31	HSP20-like chaperone
HO652385	324	SRC00573_1	*S. ratti*	IV	2.00E−53	Ribosome maturation protein SBDS, N-terminal
HO652387	837	HGC09675_1	*H. glycines*	IV	8.00E−90	Peptidase C2, calpain
HO652391	682	SSC00507_1	*S. stercoralis*	IV	6.00E−71	Basic helix-loop-helix dimerisation region bHLH
HO652393	304	SRC06206_1	*S. ratti*	IV	1.00E−11	Lysosome-associated membrane glycoprotein (Lamp)/CD68
HO652397	702	SSC03354_1	*S. stercoralis*	IV	4.00E−80	Ankyrin
HO652402	806	SRC01740_1	*S. ratti*	IV	1.00E−105	TRAF-like
HO652403	702	SSC01995_1	*S. stercoralis*	IV	1.00E−36	NLI interacting factor
HO652411	638	AAC00359_1	*A. cantonensis*	V	4.00E−39	Neurotransmitter-gated ion-channel
HO652429	713	SRC03434_1	*S. ratti*	IV	1.00E−96	Alpha/beta hydrolase fold-1
HO652446	591	PTC02320_1	*P. trichosuri*	IV	6.00E−45	Zinc finger, C3HC4 RING-type
HO652452	642	ACC01684_2	*A. caninum*	V	7.00E−42	Globin-like
HO652470	681	PTC01361_1	*P. trichosuri*	IV	2.00E−23	Bicarbonate transporter, eukaryotic
HO652471	586	SRC00877_1	*S. ratti*	IV	2.00E−99	NADH:ubiquinone oxidoreductase, 51 kDa subunit
HO652478	385	SSC01554_1	*S. stercoralis*	IV	2.00E−41	Neuroendocrine 7B2 precursor
HO652504	687	CRC01991_1	*C. remanei*	V	1.00E−47	Oxysterol-binding protein
HO652510	481	SSC05747_1	*S. stercoralis*	IV	1.00E−44	Barrier to autointegration factor, BAF
HO652512	799	SRC00306_1	*S. ratti*	IV	1.00E−152	14-3-3 protein
HO652514	263	SRC02616_1	*S. ratti*	IV	2.00E−50	C2 calcium-dependent membrane targeting
HO652517	526	SSC02701_1	*S. stercoralis*	IV	1.00E−75	Histone H2B
HO652520	545	CBC03783_1	*C. brenneri*	V	2.00E−41	Glycosyl transferase, group 1
HO652521	479	CSC01296_1	*Caenorhabditis sp.*	V	1.00E−21	RhoGAP
HO652553	286	SSC00283_1	*S. stercoralis*	IV	4.00E−29	Heat-shock protein Hsp90
HO652559	336	SSC02701_1	*S. stercoralis*	IV	5.00E−36	Histone H2B
HO652574	361	SRC08538_1	*S. ratti*	IV	9.00E−31	L3Nie Ag (SvL3Nie-2)
HO652576	666	SSC00003_1	*S. stercoralis*	IV	1.00E−86	Astacin-like metalloproteinase
HO652580	406	MHC11486_1	*M. hapla*	IV	1.00E−07	Amino acid/polyamine transporter I
HP429054	589	HBC06265_1	*H. bacteriophora*	V	3.00E−47	Globin-like protein
HP429057	461	SSC01535_1	*S. stercoralis*	IV	3.00E−19	S. stercoralis Hsp20 (SvHsp20-Ss2)
HP429059	565	ASC17349_1	*A. suum*	III	2.00E−23	A. suum Hsp20 (SvHsp20-As1)
HP429060	508	SSC00303_1	*S. stercoralis*	IV	2.00E−15	Lipase, class 2
HP429061	455	SSC00007_1	*S. stercoralis*	IV	7.00E−68	Aminotransferase, class I and II
HP429062	1558	OOC00027_4	*O. ostertagi*	V	0	Cytochrome *c* oxidase, subunit I
HP429068	655	SRC08538_1	*S. ratti*	IV	7.00E−70	L3Nie Ag (SvL3Nie-1)
HP429076	762	SSC02252_1	*S. stercoralis*	IV	1.00E−122	EF-hand
HP429077	441	SRC00553_1	*S. ratti*	IV	1.00E−35	Calcium-binding EF-hand
HP429078	524	TLC00048_1	*T. leonina*	III	3.00E−62	Cytochrome *c* oxidase, subunit III
HP429079	628	SRC00445_1	*S. ratti*	IV	6.00E−97	EF-hand
HP429083	889	SSC00456_1	*S. stercoralis*	IV	1.00E−70	Proteinase inhibitor I33, aspin
HP429085	863	CJC01127_2	*C. japonica*	V	5.00E−45	NADH:ubiquinone/plastoquinone oxidoreductase
HP429086	480	ASC00025_17	*A. suum*	III	4.00E−76	Cytochrome *c* oxidase subunit II C-terminal
HP429088	417	SRC04160_1	*S. ratti*	IV	4.00E−42	Light chain 3 (LC3)
HP429091	661	SSC01535_1	*S. stercoralis*	IV	4.00E−78	S. stercoralis Hsp20 (SvHsp20-Ss1)
HP429092	1322	SSC05809_1	*S. stercoralis*	IV	2.00E−62	Methyltransferase type 11
HP429094	277	NAC00065_1	*N. americanus*	V	3.00E−16	Cytochrome b/b6, C-terminal
HP429095	589	ASC24228_1	*A. suum*	III	2.00E−19	ATPase, F0 complex, subunit A

Genus designations used in the table are as follows: *A. caninum*; *Ancylostoma caninum*, *A. cantonensis*; *Angiostrongylus cantonensis*, *A. ceylanicum*; *Ancylostoma ceylanicum*, *A. suum*; *Acaris suum*, *C. brenneri*; *Caenorhabditis brenneri*, *C. japonica*; *Caenorhabditis japonica*, *C. remanei*; *Caenorhabditis remanei*, *H. bacteriophora*; *Heterorhabditis bacteriophora*, *H. glycines*; *Heterodera glycines*, *L. sigmodontis*; *Litomosoides sigmodontis*, *M. hapla*; *Meloidogyne hapla*, *M. javanica*; *Meloidogyne javanica*, *N. americanus*; *Necator americanus*, *O. ostertagi*; *Ostertagia ostertagi*, *P. trichosuri*; *Parastrongyloides trichosuri*, *S. ratti*; *Strongyloides ratti*, *S. stercoralis*; *Strongyloides stercoralis*, *T. leonina*; *Toxascaris leonina*, *X. index*; *Xiphinema index*.

Table 3
S. venezuelensis L3 ESTs with significant annotation against NCBI non-redundant protein database.

S. venezuelensis (singleton/contig)		Top hit in the NCBI non-redundant protein database (blastx)				Top hit in Nembase4 (tblastx)			
NCBI accession	Length (bp)	NCBI accession	Best identity descriptor	Organism	E-value	Identifier	Organism	Clade	E-value
HO652462	820	NP_501872.1	hypothetical protein F01G10.6	*C. elegans*	3.00E−12	N/F[a]	–	–	–
HO652207	396	XP_002636737.1	Hypothetical protein CBG23460	*C. briggsae*	4.00E−15	PTC02337_1	*P. trichosuri*	IV	2.00E−21
HO652218	448	XP_002633793.1	Hypothetical protein CBG03485	*C. briggsae*	6.00E−22	HCC05184_1	*H. contortus*	V	4.00E−33
HO652251	849	XP_002632491.1	CBR-CCG-1 protein	*C. briggsae*	2.00E−49	SRC00347_1	*S. ratti*	IV	1.00E−140
HO652337	409	XP_001892281.1	hypothetical protein	*B. malayi*	6.00E−38	PPC05674_1	*P. pacificus*[b]	V	8.00E−50
HO652351	463	XP_002631908.1	hypothetical protein CBG07885	*C. briggsae*	2.00E−37	PTC00166_1	*P. trichosuri*	IV	5.00E−53
HO652377	395	XP_001902589.1	putative salt tolerance protein	*B. malayi*	5.00E−19	PTC04384_1	*P. trichosuri*	IV	4.00E−61
HO652412	835	XP_002645282.1	CBR-AJM-1 protein	*C. briggsae*	3.00E−09	SSC03769_1	*S. stercoralis*	IV	8.00E−65
HO652449	581	NP_499054.1	TransThyretin-Related family domain family member (ttr-5)	*C. elegans*	9.00E−33	SRC01281_1	*S. ratti*	IV	2.00E−84
HO652459	286	NP_510509.2	hypothetical protein F09B12.3	*C. elegans*	1.00E−14	SRC04118_1	*S. ratti*	IV	2.00E−34
HO652491	650	XP_001902568.1	hypothetical protein Bm1_55555	*B. malayi*	1.00E−27	SSC01022_1	*S. stercoralis*	IV	2.00E−85
HO652499	797	NP_505173.2	hypothetical protein F52E1.13	*C. elegans*	3.00E−43	CRC02974_1	*C. remanei*	V	5.00E−20
HO652537	528	NP_499054.1	TransThyretin-Related family domain family member (ttr-5)	*C. elegans*	2.00E−30	SRC01281_1	*S. ratti*	IV	4.00E−78
HO652548	533	XP_002646626.1	Hypothetical protein CBG11056	*C. briggsae*	8.00E−10	SRC02345_1	*S. ratti*	IV	3.00E−57
HP429066	2081	NP_492698.2	hypothetical protein ZC247.1	*C. elegans*	1.00E−71	SSC03002_1	*S. stercoralis*	IV	6.00E−72
HP429084	856	CAR63582.1	Conserved Cystein/Glycine domain protein	*A. cantonensis*	1.00E−41	SRC00347_1	*S. ratti*	IV	1.00E−129

S. venezuelensis L3i ESTs that did not hit in NEMABASE4 or ESTs which had matches to NEMABASE4 ESTs without annotation, were further analysed against NCBI non-redundant protein database. Sixteen EST were given annotation by this search.
[a] N/F: no hit in NEMABASE4.
[b] *Pristionchus pacificus*.

comprised the unique sequences, which were compared against NEMBASE4 (http://www.nematodes.org/ nembase4/), using tBLASTx. ESTs that did not hit were further compared with the National Center for Biotechnology Information (NCBI) non-redundant protein database using BLASTx (cut-off: E<1e−5), and NCBI EST database using BLASTn (cut-off: E<1e−10). The sequences of the transcripts in the

Hsp20

```
SvHsp20-Ss1    1:MAANNNNPSDSTDSSTXSNEEHHXERTXSYY-APSKKDDKSSAFVFSTLLEXGKDQIVCD 59
SvHsp20-Ss2    1:----------------------------N-FTMSTSS-E-------K-L-VW-------D 14
SvHsp20-As1    1:IKXLR-------------H------RCVFPSAIPMLIHTTNSI--LNDLESSLNPRHVXS 39
                                          .       .       .       *       . .

SvHsp20-Ss1   60:WPLNVKNDGLFKSKELNDKITLTLDCRXFDPQDIQVSVXGERVGIHCEHPKRKNSTT-CE 118
SvHsp20-Ss2   15:WPLSHSEDGVFTSKEIDGKIGITVDCKLFKDKEVNVIVDKDKIDIHCLHEEVEKSGLVCK 74
SvHsp20-As1   40:LKIIRDEGVSITNEGISLKFDVSQ----FKXEELSINVVDGVLVIEGKHEQMDDGKGIVS 95
                 ...   ... ......  *.  . ..  *.  .  . *      *.. *.    .   .

SvHsp20-Ss1  119:RKISRTYKXPQCYDINTLQHKVNSSGELII---------TANRTXRT---          156
SvHsp20-Ss2   75:REISRCYRLPATLDPKTVKHSLKN-GELII---------TVEK--KA---          109
SvHsp20-As1   96:RHFIRKFRLPENLKAEDIKSELSKEGMLAIEGKCLDHEKTKVKSIPIDVK          145
                 * ..* ...*  ..  . . .  *.*.*        *  .
```

L3Nie

```
SvL3Nie-1      1:FDISKYKGNNKFSNKIFDQIWKGYNYDSDKQNKFVDMKRRFLLETNKYRRAQGVPNLVVD 60

SvL3Nie-1     61:SGLAAKAQKYAEYLAQIRQLVHDRRNSIEKTGENLAFGSPLISHLAVKKWYDEIELYDFN 120
SvL3Nie-2      1:                          NQKNKLGENLAFASPRIAHIGVKGWYDEVKDYNFN 35
                                              * ****** ** * *  ** ****   * **

SvL3Nie-1    121:RPGFSSATGHFTQLVWKDSRKAGFGVAVSSDGKGVYVVCKYTPPGNYNNKYSENVKRLSA 180
SvL3Nie-2     36:KQGFRHGIGHFTQLVWKSSSKVGCGVA--AGSKGVFTVCKYSPAGNLMGAFEKNVSPKKA 93
                    **    ********* * * * ***     ***  **** * **       **    *

SvL3Nie-1    181:TKPSSKPKRRS
```

Fig. 1. Comparison of predicted amino acid sequences between three Hsp20s and two L3Nie antigens. In *S. venezuelensis* ESTs, three different Hsp20 and two L3Nie were found. In order to clarify the difference between these ESTs, they were aligned against each other by using the GENETYX-WIN software (GENETYX CORPORATION, Tokyo, Japan). Identical residues are marked with an asterisk, and conserved residues between two Hsp20s are marked with a dot. SvHsp20-Ss1 showed 40% identity to SvHsp20-Ss2. SvHsp20-As1 was found to have 29% identity with SvHsp20-Ss2, but no significant similarity with SvHsp20-Ss1. Identity between SvL3Nie-1 and 2 was 56%. Accession numbers for each genes: SvHSP20-Ss1; HP429091, SvHSP20-Ss2; HP429057, SvHSP20-As1; HP429059, SvL3Nie-1; HP429068, SvL3Nie-2; HO652574.

present study have been deposited into the GenBank under accession numbers HO652177–HO652584 and HP429054–HP429095.

2.5. Reverse transcriptase-polymerase chain reaction (RT-PCR)

RT-PCR was performed with worms of different developmental stages; infective larvae (L3i), tissue-migrating larvae (L3tm), lung larvae (LL3), and parasitic adult worms. For RNA isolation, worms were crushed manually using a freeze-crushing apparatus (SK Mill, Tokken, Chiba, Japan), followed by isolation with TRIzol reagent. After treatment with DNase I (Ambion, Austin, TX, USA), concentration of RNA was measured using a Quant-iT assay kit (Invitrogen). cDNA was synthesized from 1 μg of total RNA by reverse transcription in 100 μl reaction using PrimeScript 1st strand cDNA Synthesis Kit (Takara Bio, Shiga, Japan).

For 63 selected genes, PCR primers were designed to have theoretical Tm of 57–63 °C and amplicon sizes of 200–500 bp. One microliter of the prepared cDNA preparation was used for PCR amplification. The amplification program was as follows; initial denaturation at 94 °C for 2 min, 30 cycles of denaturation at 94 °C for 45 s, annealing 58 °C for 45 s and elongation at 68 °C for 30 s, followed by a final extension at 68 °C for 7 min. Five microliter of the PCR products was mixed with 1 μl of EZ-VISION DNA dye/buffer (AMRESCO, Solon, OH, USA), run on 1% agarose gel, then visualized by UV transillumination and photographed.

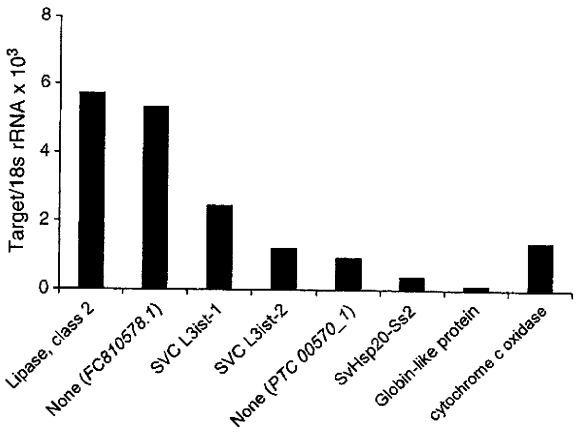

Fig. 2. Expression analysis of abundant transcripts in infective larvae. Quantification of transcripts was achieved by real-time PCR using gene-specific primer sets for the top 8 sequences (Table 4). The gene for a class 2 lipase was the most abundantly transcribed in L3i, which was followed by novel genes of unknown functions. The target values were normalized to 18S rRNA expression. Accession numbers for each genes: lipase; HP429060, *FC810578.1*; HP429073, SVC L3ist-1; HP429055, SVC L3ist-2; , HP429056, *PTC 00570_1*; HP429058, SvHsp20-Ss2; HP429057, Globin-like protein; HP429054, cytochrome *c* oxidase; HP429062.

2.6. Real-time PCR analyses

Expression of selected transcripts was analyzed in real-time PCR. The regions amplified with each primer sets were shown in Table 1. Total RNA was extracted from different stages of larvae as described above, and cDNA was generated from 400 ng of RNA using Prime-Script 1st strand cDNA Synthesis Kit (Takara Bio). Real-time PCR was then performed with an ABI PRISM 7000 Sequence Detection Systems and a Power SYBR Green PCR Master Mix (Applied Biosystems). Relative quantification was assessed by normalizing the amount of the target transcript to 18S ribosomal RNA gene.

3. Results

A cDNA library was constructed from infective larvae of *S. venezuelensis*. A total of 500 clones were sequenced producing 408 high quality ESTs (250 bp cut-off) with an average of 490 ± 164 bp. Assembling the 408 ESTs resulted in 42 contigs (288 ESTs) and 120

Table 4
The most abundant transcripts in *S. venezuelensis* L3i cDNA library.

S. venezuelensis (singleton/contig)		Blast top hit against NEMABASE4			
NCBI accession	Number of clones	Identifier	Organism	E-value	Associated annotation
HP429060	38	SSC00303_1	*S. stercoralis*	2.00E−15	Lipase, class 2
HP429056	33	Novel[a] (SVC L3ist-2)	–	–	–
HP429054	29	HBC06265_1	*H. bacteriophora*	3.00E−47	Globin-like protein
HP429055	27	Novel[a] (SVC L3ist-1)	–	–	–
HP429057	26	SSC01535_1	*S. stercoralis*	3.00E−19	S. stercoralis Hsp20 (SvHsp20-Ss2)
HP429073	14	FC810578.1[b]	*S. ratti*	5.00E−13	None
HP429058	10	PTC00570_1	*P. trichosuri*	3.00E−29	None
HP429062	8	OOC00027_4	*O. ostertagi*	0	Cytochrome *c* oxidase, subunit I
HP429064	7	Novel[a]	–	–	–
HP429079	6	SRC00445_1	*S. ratti*	6.00E−97	EF-hand
HP429066	5	SSC03002_1	*S. stercoralis*	6.00E−72	None
HP429070	5	SRC01349_1	*S. ratti*	2.00E−19	None
HP429075	5	SSC00031_1	*S. stercoralis*	5.00E−70	None
HP429076	4	SSC02252_1	*S. stercoralis*	1.00E−122	EF-hand
HP429085	4	CJC01127_2	*C. japonica*	5.00E−45	NADH:ubiquinone/plastoquinone oxidoreductase
HP429072	4	SRC01349_1	*S. ratti*	2.00E−22	None
HP429067	4	Novel[a]	–	–	–
HP429069	4	Novel[a]	–	–	–
HP429059	3	ASC17349_1	*A. suum*	2.00E−23	A. suum Hsp20 (SvHsp20-As1)
HP429068	3	SRC08538_1	*S. ratti*	7.00E−70	L3Nie Ag (SvL3Nie-1)
HP429084	3	SRC00347_1	*S. ratti*	1.00E−129	None
HP429081	3	SRC07826_1	*S. ratti*	4.00E−37	None
HP429074	3	SSC04537_1	*S. stercoralis*	2.00E−07	None
HP429087	3	Novel[a]	–	–	–
HP429065	3	Novel[a]	–	–	–

[a] Novel; No hits were found in major public databases.
[b] All hits shown here were found against Nembase4 except for FC810578.1, which was found a match in NCBI EST database only.

singletons. tBLASTx analysis against NEMABASE4, a comprehensive resource for nematode transcriptome analysis holding 679,480 nematode EST, resulted in 114 (70.4%) *S. venezuelensis* L3i ESTs showing significant (E<1e−5) matches to nematode EST, in which associated annotation was given to 68 sequences (Table 2).

S. venezuelensis L3i ESTs that did not hit in NEMABASE4 and the ones which had matches to NEMABASE4 ESTs without annotation, were further analyzed by BLASTx against the NCBI non-redundant protein databases. This search yielded 16 more genes with description (Table 3). Thus in total, 84 ESTs resulted in significant annotation against the major public databases. It should be noted that most of the hits in NEMABASE4 were genes of clade IV nematode, and a majority of the clade IV hits were with genes from *Strongyloides* (Tables 2 and 3).

Some *S. venezuelensis* L3i ESTs shown in Table 2 hit the same sequences in databases. For example, HP429091 and HP429057 hit *S. stercoralis* Hsp20 (SSC01535_1), and HP429068 and HO652574 hit *S. ratti* L3Nie Ag (SRC08538_1). Sequence alignment of these ESTs revealed that they differed significantly from each other (Fig. 1). Therefore, they were considered as different gene products and designated as shown in Fig. 1.

Of 162 *S. venezuelensis* L3i ESTs, 47 gave no hits in NCBI databases or NEMABASE4 in BLASTx and tBLASTx, respectively. We compared these sequences with NCBI EST division in BLASTn to find 7 more hits (E<1e−10). Thus of 162 unique sequences, 37 (22.3%) had no hits against NCBI or NEMABASE4, indicating that these were novel genes.

Matched transcripts with significant annotation (84 sequences) could be grouped into some categories: genes for proteins involved in oxidative phosphorylation, structural proteins, heat-shock proteins, neuromuscular proteins, and immunodominant proteins. Interesting transcripts were also found such as calpain (HO652387, Table 2), astacin-like metalloproteinase (HO652576, Table 2), salt tolerance protein (HO652377, Table 3), DNA repair protein (HO652242, Table 2), and autophagy-related LC3 (HP429088, Table 2).

The most abundant transcripts in *S. venezuelensis* infective larva, estimated from the frequency of clones, contained class 2 lipase, globin-like protein, and small heat-shock protein 20, SvHsp20-Ss2, similar to *S. stercoralis* Hsp20. However, a number of abundant transcripts had no hits even against NCBI EST using BLASTn (Table 4), suggesting that infective larvae probably express a number of species-specific genes. In order to examine the relative amount of expression of these seemingly abundant transcripts in L3i, we performed real-time PCR for the top 8 sequences containing 4 unannotated ESTs. We found that the gene for a class 2 lipase was the most abundantly transcribed in L3i, which was followed by novel genes and genes of unknown functions (Fig. 2). Two genes, *S. venezuelensis* L3i-specific transcript 1 and 2 (SVC L3ist-1 and SVC L3ist-2), had no hits in nucleotide databases by BLASTn analysis, indicating that these were novel genes.

Because infective larvae have to survive stressful environment, we examined in real-time PCR the gene expression of heat-shock proteins and energy-related proteins in different developmental stages. Expression profile of the heat-shock proteins differed from each other. As shown in Table 2, we obtained one Hsp90 and three Hsp20

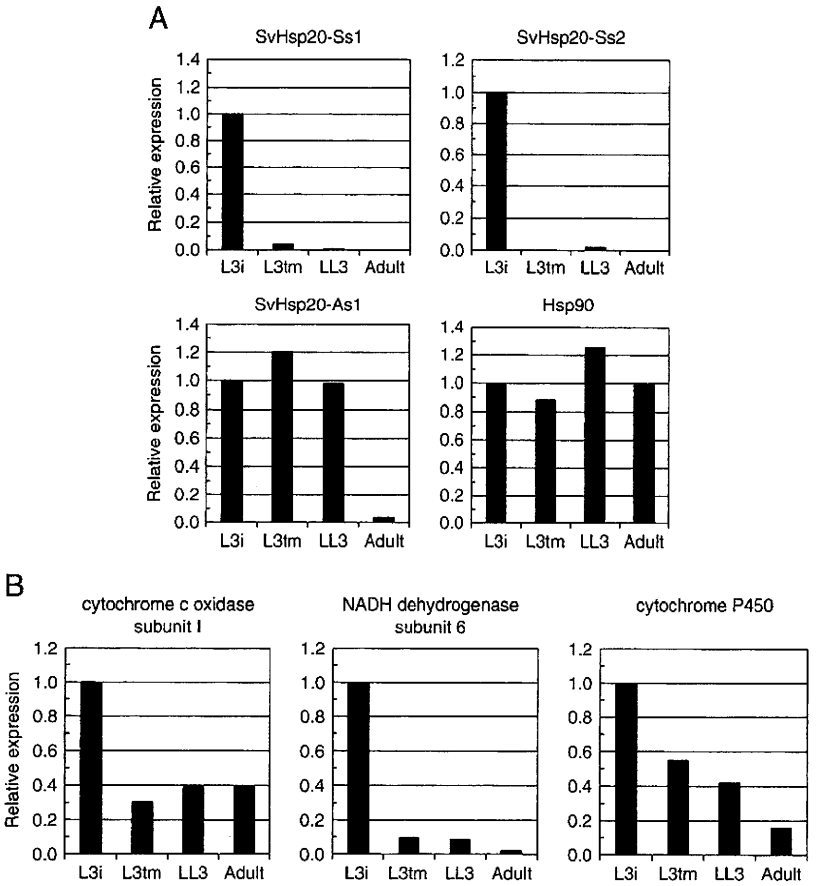

Fig. 3. Comparison of mRNA expression in developmental stages. Real-time PCR was performed with infective larvae (L3i), tissue-migrating larvae (L3tm), lung larvae (LL3) and adult female worms. (A) Expression profile of the heat-shock proteins. Hsp90 was evenly expressed through all developmental stages, while the expression of SvHsp20-As1 was decreased in adult worm. SvHsp20-Ss1 was expressed only in the infective larva stage differed from each other. (B) Gene expression of energy-related proteins. Genes, including cytochrome c oxidase subunit I, NADH dehydrogenase subunit 6, and cytochrome P450, were most actively transcribed in the infective larva stage. Relative expression of the target genes was assessed by normalizing to 18S rRNA expression. Gene expression in L3i was defined as 1.0. Accession numbers for each genes: SvHsp20-Ss1; HP429091, SvHsp20-Ss2; HP429057, SvHsp20-As1; HP429059, Hsp90; HO652553, cytochrome c oxidase; HP429062, NADH dehydrogenase; HO652258, cytochrome P450; HO652210.

sequences. Since these three Hsp20 (HP429091, HP429057, and HP429059) differed significantly from each other (Fig. 1), they were referred to as SvHsp20-Ss1, SvHsp20-Ss2, and SvHsp20-As1, respectively. While Hsp90 was expressed evenly from infective larvae to parasitic adult females, the expression of SvHsp20-As1 decreased when the worms reached maturity. In contrast, SvHsp20-Ss1 and SvHsp20-Ss2 were expressed only in the infective larva stage (Fig. 3A).

Genes for spiration-related proteins, including cytochrome c oxidase subunit I (HP429062), NADH dehydrogenase (HO652258), and cytochrome P450 (HO652210), were most actively transcribed in the infective larva stage (Fig. 3B), suggesting that infective larvae are active in producing ATP by oxidative phosphorylation. In fact, infective larvae had batteries of well-developed mitochondria immediately under the muscular layer demonstrated by transmission electron microscopy (data not shown).

In order to identify L3i-specific transcripts, which could be the clues to the elucidation of the survival strategy of infective larvae, we compared the expression pattern along the developmental stages of 62 genes by RT-PCR, containing 57 annotated and 5 non-annotated but highly abundant genes listed in Table 4. cDNA was prepared from infective larvae (L3i), tissue-migrating larvae (L3tm), lung larvae (LL3), and parasitic adult female worms, was amplified in PCR followed by the examination on agarose gel. PCR products were successfully obtained for 52 transcripts, revealing 7 transcripts being specific for infective larva stage (Table 5).

To confirm the stage specificity of these genes, we examined the expression in real-time PCR. Among 7 L3i specific transcripts listed in Table 5, the specific expression of SvHsp20-Ss1 and SvHsp20-Ss2, has been already demonstrated in Fig. 3. As shown in Fig. 4, the expression of the remaining 5 genes was highly specific as well for infective larvae. In addition to SvHsp20-Ss1 and SvHsp20-Ss2, L3i-specific transcripts were astacin-like metalloprotease, SvL3Nie-2, an unannotated gene (*PTC 00570_1*), and two novel transcripts (SVC L3ist-1 and SVC L3ist-2). Quite interestingly, SvL3Nie-1, which is similar to SvL3Nie-2, showed different expression patterns with SvL3Nie-2. SvL3Nie-1 was expressed constitutively from L3i to tissue-migrating L3tm stage (Fig. 4).

Table 5
Expression of transcripts along developmental stages.

S. venezuelensis (singleton/contig)		Best identity descriptor
Expression	NCBI accession	
L3i only	HO652574	SvL3Nie-2
	HO652576	Astacin-like metalloproteinase
	HP429055	Novel[a] (SVC L3ist-1)
	HP429056	Novel[a] (SVC L3ist-2)
	HP429057	SvHsp20-Ss2
	HP429058	None (PTC 00570_1)[b]
	HP429091	SvHsp20-Ss1
L3i to L3tm	HP429068	SvL3Nie-1
L3i to LL3	HO652180	FMRFamide-related peptide
	HO652403	NLI interacting factor
	HO652411	Neurotransmitter-gated ion-channel
	HP429054	Globin-like protein
	HP429059	SvHsp20-As1
	HP429061	Aminotransferase, class I and II
	HP429076	EF-hand
	HP429077	Calcium-binding EF-hand
	HP429088	Light chain 3 (LC3)
L3i to adult	HO652177	Proteasome, subunit alpha/beta
	HO652206	Ammonium transporter
	HO652234	Ras small GTPase, Ras type
	HO652242	DNA repair protein (XPGC)/yeast Rad
	HO652251	C. briggsae CBR-CCG-1 protein[c]
	HO652258	NADH dehydrogenase subunit 6
	HO652261	Poly(A)-binding protein
	HO652285	beta-1,4-mannosyltransferase activity
	HO652301	Histone H1/H5
	HO652303	NIF system FeS cluster assembly, NifU, N-terminal
	HO652319	Neural proliferation differentiation control-1
	HO652339	Klarsicht/ANC-1/syne-1 homology
	HO652341	Neurotransmitter-gated ion-channel
	HO652363	Isocitrate lyase and phosphorylmutase
	HO652371	HSP20-like chaperone
	HO652385	Ribosome maturation protein SBDS, N-terminal
	HO652387	Peptidase C2, calpain
	HO652397	Ankyrin
	HO652412	*C. briggsae* CBR-AJM-1 protein[c]
	HO652449	TransThyretin-Related family domain family member[c]
	HO652459	hypothetical protein F09B12.3[c]
	HO652470	Bicarbonate transporter, eukaryotic
	HO652504	Oxysterol-binding protein
	HO652510	Barrier to autointegration factor, BAF
	HO652514	C2 calcium-dependent membrane targeting
	HO652517	Histone H2B
	HO652520	Glycosyl transferase, group 1
	HO652537	TransThyretin-Related family domain family member[c]
	HO652553	Heat-shock protein Hsp90
	HP429060	Lipase, class 2
	HP429062	Cytochrome *c* oxidase, subunit I
	HP429073	None[b]
	HP429083	Proteinase inhibitor I33, aspin
	HP429084	Putative conserved cystein/glycine domain protein[c]
	HP429092	Methyltransferase type 11

[a] Novel; No hits were found in major databases.
[b] Hits were found in NEMABASE4 with no associated annotation.
[c] Hits were found in NEMABASE4 without associated annotation. Annotation was given in NCBI NR protein database.

4. Discussion

Most cases of strongyloidiasis are subclinical, and chronic infections remain unrecognized for decades [14]. However, it might turn life-threatening when the patients are on immunosuppressive drugs [15] or have co-infections with HTLV-1 [16–18]. In severe strongyloidiasis, large numbers of infective larvae penetrate skin and intestinal mucosa causing disseminated infections. Understanding the biology of infective larvae would lead us to find a novel strategy for the control of severe infections.

Our present study on transcripts of *S. venezuelensis* infective larva revealed interesting features of their biology. First, in the present cDNA library, clones coding for lipase appeared repeatedly. Representation in a cDNA library generally reflects the abundance in the original transcriptome [19], and the real-time PCR results confirmed lipase as one of the most actively transcribed genes (Fig. 2). It appears that infective larvae of *S. venezuelensis* possibly degrade stored lipid for energy generation. Because infective larvae do not feed during wait [20], and express both an autophagosome marker LC3 (HP429088 in Table 2) and a proteasome protein (HO652177 in Table 2), infective larvae possibly depend on both the ubiquitin–proteasome system and autophagy processes for the energy sources. Recent study has revealed that autophagy regulates intracellular lipid metabolism [21], which is evoked when animals are under starvation [22–24].

Transcripts for several different heat-shock proteins were found in *S. venezuelensis* infective larvae cDNA. Hsp90, an evolutionarily conserved indispensable molecular chaperone, is involved in the folding, stabilization, activation, and assembly of a wide range of cellular proteins, playing a central role in many biological processes [25]. In *C. elegans*, Hsp90 is upregulated in dauer larvae, to which infective larvae of parasitic nematodes are often compared [26]. Our present study demonstrated that Hsp90 is abundantly and constitutively transcribed throughout the life of *S. venezuelensis* (Fig. 3A). In spite of a number of similarities between infective larvae and dauer larvae, recent comparative genomics between *C. elegans* and

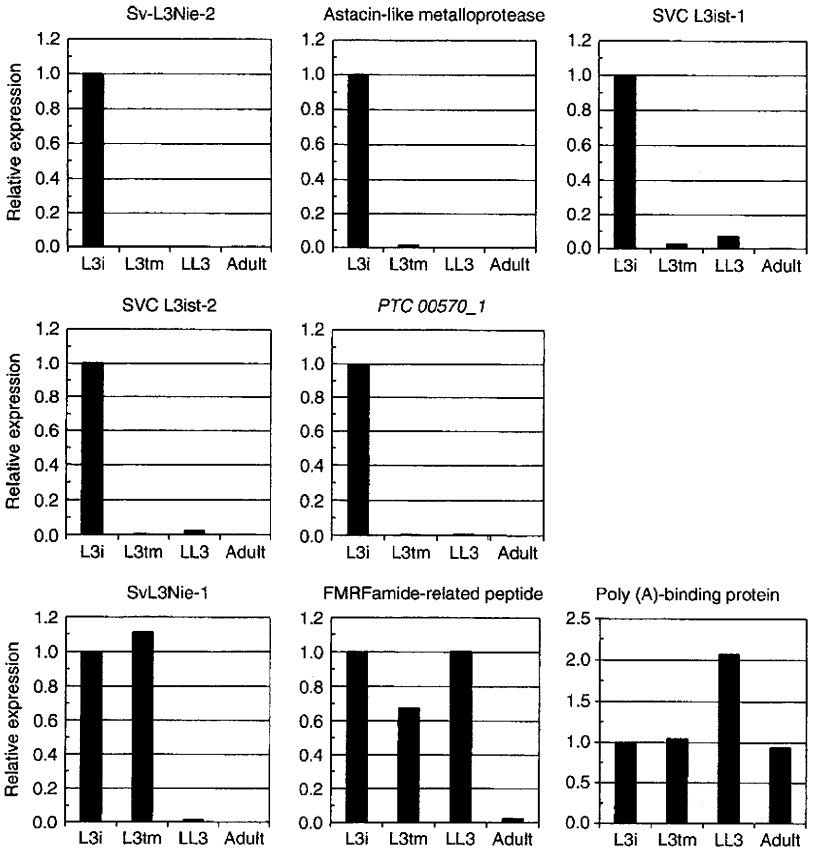

Fig. 4. Quantitative analysis of mRNA expression for infective larvae (L3i) specific transcripts. Quantitative real-time PCR validated the specific expression of six genes in infective L3 larvae. Relative expression of the target genes was assessed by normalizing to 18S rRNA expression. Gene expression in L3i was defined as 1.0. Accession number for genes analysed are as follows: Sv-L3Nie-2; HO652574, Astacin-like metalloprotease; HO652576, SVC L3ist-1 (novel gene); HP429055, SVC L3ist-2 (novel gene); HP429056, *PTC 00570_1*; HP429058, Sv-L3Nie-1; HP429068, FMR Famide-related peptide; HO652180, Poly (A)-binding protein; HO652261.

S. stercoralis has failed uncover evidence of an L3i/dauer expression signature conserved between the two species [27].

On the other hand, interesting expression patterns were observed in small heat-shock proteins, Hsp20. We found that infective larvae of *S. venezuelensis* had at least three Hsp20s, which were significantly different not only in the sequence but in the expression pattern along the developmental stages as well (Fig. 3A). In mammals, Hsp20 protects cells from the aggregation of denatured proteins, and is abundantly expressed in smooth muscle cells and cardiomyocytes [28,29]. In parasitic nematodes, small heat-shock proteins have been reported to have a role in muscle cells and muscle contraction [30]. Therefore these Hsp20 might be involved in different muscular functions, or they might have totally different roles in *S. venezuelensis*.

Upon infection, infective larvae must penetrate skin as quickly as possible. Infective larvae of *S. venezuelensis* have a zinc metalloprotease activity, which has been assumed to play a major role in skin penetration [12]. This metalloprotease activity at 40 kDa is presumably a *S. venezuelensis* homologue of Ss40 of *S. stercoralis*, a zinc metalloprotease deployed by infective larvae [31,32]. Recent study identified an astacin-like metalloprotease transcript in infective larvae of *S. stercoralis*, which has been referred to as 'strongylastacin' [33], to which one of the transcripts in the present study (HO652576) is highly homologous. The expression of this transcript is specific for infective larva stage, which perfectly matches to the metalloprotease activity previously reported [12].

The most significant results in this study were that the substantial portion of transcripts of *S. venezuelensis* infective larvae contained novel sequences. Especially, novel transcripts, SVC L3ist-1 and SVC L3ist-2, were abundantly expressed and they were infective larva-specific (Table 5, Fig. 4). We could not find similar sequences in public nucleotide databases, even against NEMABESE4, the most comprehensive resource for nematode EST analysis. Because NEMABESE4 contains EST data on *S. stercoralis* as well as *S. ratti*, these two transcripts should be not only stage-specific but species-specific molecules. Transcriptome analysis of *Ancylostoma caninum* has revealed that more than 80% of infective larva-specific transcripts (66 out of 78) are species-specific [34]. Comparative genomics among hookworms and *Srtongyloides* nematodes, that produce tissue penetrating infective larvae, should be one of the most exciting issues in the field of parasitology.

Apart from the biology of *S. venezuelensis* infective larvae, we could identify transcripts for candidate antigens for immunodiagnosis. We found two different transcripts homologous to *S. stercoralis* L3Nie antigen (SvL3Nie-1 and SvL3Nie-2) and proteinase inhibitor I33, which is similar to *Onchocerca volvulus* immunodominant antigen Ov33 (HP429083). L3Nie antigen is a member of the Ancylostoma Secretory Protein family, which was cloned with a patient serum [35], and has been shown to be useful in the diagnosis of strongyloidiasis [36]. Ov33, on the other hand, is recognized by more than 90% of onchocerciasis patient sera and has been used for immunodiagnosis as a single protein or fusion protein [37,38]. Gold standard for the diagnosis method for strongyloidiasis is the stool examination, however, the sensitivity of detecting larvae is not enough especially for chronic infections in immunocompetent hosts [39,40]. Because Ov33 homologue and L3Nie antigen appear to be abundantly transcribed in larvae, the combined use of the two antigens in immunodiagnosis might improve the sensitivity and specificity

significantly. Therefore further analysis is required of these antigens with strongyloidiasis patient sera.

5. Conclusions

A total of 408 EST were obtained from a cDNA library of *S. venezuelensis* infective larvae. Most abundant transcripts are those for lipase, respiration enzymes, and heat-shock proteins, however they contained 37 novel sequences which cannot be found in public nucleotide databases. Of seven transcripts which are infective larvae stage-specific, three have been unannotated and two were novel. Further research on these novel genes will clarify the biology of the infective larva.

Acknowledgements

This work was supported by grants from the Ministry of Education, Culture, Sports, Science and Technology of Japan (Grant-in-Aid for Scientific Research C 21590466, Grant-in-Aid for Scientific Research on Priority Areas 'Matrix of Infection Phenomena' 21022041), the Ministry of Health, Labour and Welfare (H20-Shinko-Ippan-016, H21-Kokui-Shitei-004), and the Japan Health Sciences Foundation (KHA2031).

References

[1] Román-Sánchez P, Pastor-Guzmán A, Moreno-Guillén S, Igual-Adell R, Suñer-Generoso S, Tornero-Estébanez C. High prevalence of *Strongyloides stercoralis* among farm workers on the Mediterranean coast of Spain: analysis of the predictive factors of infection in developed countries. Am J Trop Med Hyg 2003;69:336–40.
[2] Safdar A, Malathum K, Rodriguez SJ, Husni R, Rolston KV. Strongyloidiasis in patients at a comprehensive cancer center in the United States. Cancer 2004;100:1531–6.
[3] Hirata T, Uchima N, Kishimoto K, Zaha O, Kinjo N, Hokama A, et al. Impairment of host immune response against *Strongyloides stercoralis* by human T cell lymphotropic virus type 1 infection. Am J Trop Med Hyg 2006;74:246–9.
[4] Couillault C, Pujol N, Reboul J, Sabatier L, Guichou JF, Kohara Y, et al. TLR-independent control of innate immunity in *Caenorhabditis elegans* by the TIR domain adaptor protein TIR-1, an ortholog of human SARM. Nat Immunol 2004;5:488–94.
[5] Pujol N, Zugasti O, Wong D, Couillault C, Kurz CL, Schulenburg H, et al. Anti-fungal innate immunity in *C. elegans* is enhanced by evolutionary diversification of antimicrobial peptides. PLoS Pathog 2008;4:e1000105.
[6] Hotez PJ, Bethony J, Bottazzi ME, Brooker S, Diemert D, Loukas A. New technologies for the control of human hookworm infection. Trends Parasitol 2006;22:327–31.
[7] Suarez VH. Helminthic control on grazing ruminants and environmental risks in South America. Vet Res 2002;33:563–73.
[8] De Lange HJ, Lahr J, Van der Pol JJ, Wessels Y, Faber JH. Ecological vulnerability in wildlife: an expert judgment and multicriteria analysis tool using ecological traits to assess relative impact of pollutants. Environ Toxicol Chem 2009;28:2233–40.
[9] Maruyama H, Nawa Y, Ohta N. *Strongyloides venezuelensis*: binding of orally secreted adhesion substances to sulfated carbohydrates. Exp Parasitol 1998;89:16–20.
[10] Korenaga M, Nawa Y, Mimori T, Tada I. *Strongyloides ratti*: the role of enteral antigenic stimuli by adult worms in the generation of protective immunity in rats. Exp Parasitol 1983;55:358.
[11] Maruyama H, Yabu Y, Yoshida A, Nawa Y, Ohta N. A role of mast cell glycosaminoglycans for the immunological expulsion of intestinal nematode, *Strongyloides venezuelensis*. J Immunol 2000;164:3749–54.
[12] Maruyama H, Nishimaki A, Takuma Y, Kurimoto M, Suzuki T, Sakatoku Y, et al. Successive changes in tissue migration capacity of developing larvae of an intestinal nematode, *Strongyloides venezuelensis*. Parasitology 2006;132:1–8.
[13] Wertheim G. Growth and development of *Strongyloides venezuelensis* Brumpt, 1934 in the albino rat. Parasitology 1970;61:381–8.
[14] Gill GV, Welch E, Bailey JW, Bell DR, Beeching NJ. Chronic *Strongyloides stercoralis* infection in former British Far East prisoners of war. Q J Med 2004;97:789–95.
[15] Keiser PB, Nutman TB. *Strongyloides stercoralis* in the immunocompromised population. Clin Microbiol Rev 2004;17:208–17.
[16] Yamaguchi K, Takatsuki K. Adult T cell leukaemia-lymphoma. Baillières Clin Haematol 1993;6:899–915.
[17] Verdonck K, González E, Van Dooren S, Vandamme AM, Vanham G, Gotuzzo E. Human T-lymphotropic virus 1: recent knowledge about an ancient infection. Lancet Infect Dis 2007;7:266–81.
[18] Marcos LA, Terashima A, Dupont HL. Strongyloides hyperinfection syndrome: an emerging global infectious disease. Trans R Soc Trop Med Hyg 2008;102:314–8.
[19] Audic S, Claverie JM. The significance of digital gene expression profiles. Genome Res 1997;7:986–95.
[20] Ashton FT, Zhu X, Boston R, Lok JB, Schad GA. *Strongyloides stercoralis*: amphidial neuron pair ASJ triggers significant resumption of development by infective larvae under host-mimicking in vitro conditions. Exp Parasitol 2007;115:92–7.
[21] Singh R, Kaushik S, Wang Y, Xiang Y, Novak I, Komatsu M, et al. Autophagy regulates lipid metabolism. Nature 2009;458:1131–5.
[22] Mizushima N, Yamamoto A, Matsui M, Yoshimori T, Ohsumi Y. In vivo analysis of autophagy in response to nutrient starvation using transgenic mice expressing a fluorescent autophagosome marker. Mol Biol Cell 2004;15:1101–11.
[23] Kuma A, Hatano M, Matsui M, Yamamoto A, Nakaya H, Yoshimori T, et al. The role of autophagy during the early neonatal starvation period. Nature 2004;432:1032–6.
[24] Shibata M, Yoshimura K, Tamura H, Ueno T, Nishimura T, Inoue T, et al. LC3, a microtubule-associated protein1A/B light chain3, is involved in cytoplasmic lipid droplet formation. Biochem Biophys Res Commun 2010;393:274–9.
[25] Nollen EA, Morimoto RI. Chaperoning signaling pathways: molecular chaperones as stress-sensing 'heat shock' proteins. J Cell Sci 2002;115:2809–16.
[26] Ogawa A, Streit A, Antebi A, Sommer RJ. A conserved endocrine mechanism controls the formation of dauer and infective larvae in nematodes. Curr Biol 2009;19:67–71.
[27] Mitreva M, McCarter JP, Martin J, Dante M, Wylie T, Chiapelli B, et al. Comparative genomics of gene expression in the parasitic and free-living nematodes *Strongyloides stercoralis* and *Caenorhabditis elegans*. Genome Res 2004;14:209–20.
[28] Fan GC, Ren X, Qian J, Yuan Q, Nicolaou P, Wang Y, et al. Novel cardioprotective role of a small heat-shock protein, Hsp20, against ischemia/reperfusion injury. Circulation 2005;111:1792–9.
[29] Salinthone S, Tyagi M, Gerthoffer WT. Small heat shock proteins in smooth muscle. Pharmacol Ther 2008;119:44–54.
[30] Raghavan N, Ghosh I, Eisinger WS, Pastrana D, Scott AL. Developmentally regulated expression of a unique small heat shock protein in *Brugia malayi*. Mol Biochem Parasitol 1999;104:233–46.
[31] McKerrow JH, Brindley P, Brown M, Gam A, Stanton C, Neva FA. *Strongyloides stercoralis*: identification of a protease that facilitates penetration of the skin by the infective larvae. Exp Parasitol 1990;70:134–43.
[32] Brindley PJ, Gam AL, McKerrow JH, Neva FA. Ss40: the zinc endopeptidase secreted by infective larvae of *Strongyloides stercoralis*. Exp Parasitol 1995;80:1–7.
[33] Gomez Gallego S, Loukas A, Slade RW, Neva FA, Varatharajalu R, Nutman TB, et al. Identification of an astacin-like metallo-proteinase transcript from the infective larvae of *Strongyloides stercoralis*. Parasitol Int 2005;54:123–33.
[34] Wang Z, Abubucker S, Martin J, Wilson RK, Hawdon J, Mitreva M. *Ancylostoma caninum* transcriptome and exploring nematode parasitic adaptation. BMC Genomics 2010;11:307.
[35] Ravi V, Ramachandran S, Thompson RW, Andersen JF, Neva FA. Characterization of a recombinant immunodiagnostic antigen (NIE) from *Strongyloides stercoralis* L3-stage larvae. Mol Biochem Parasitol 2002;125:73–81.
[36] Ramanathan R, Burbelo PD, Groot S, Iadarola MJ, Neva FA, Nutman TB. A luciferase immunoprecipitation systems assay enhances the sensitivity and specificity of diagnosis of *Strongyloides stercoralis* infection. J Infect Dis 2008;198:444–51.
[37] Lucius R, Kern A, Seeber F, Pogonka T, Willenbucher J, Taylor HR, et al. Specific and sensitive immunodiagnosis of onchocerciasis with a recombinant 33 kD *Onchocerca volvulus* protein (Ov33). Trop Med Parasitol 1992;43:139–45.
[38] Nde PN, Pogonka T, Bradley JE, Titanji VP, Lucius R. Sensitive and specific serodiagnosis of onchocerciasis with recombinant hybrid proteins. Am J Trop Med Hyg 2002;66:566–71.
[39] Sato Y, Kobayashi J, Toma H, Shiroma Y. Efficacy of stool examination for detection of *Strongyloides* infection. Am J Trop Med Hyg 1995;53:248–50.
[40] Siddiqui AA, Berk SL. Diagnosis of *Strongyloides stercoralis* infection. Clin Infect Dis 2001;33:1040–7.

Notch2 signaling is required for proper mast cell distribution and mucosal immunity in the intestine

Mamiko Sakata-Yanagimoto,[1,2] Toru Sakai,[3] Yasuyuki Miyake,[1] Toshiki I. Saito,[2,4] Haruhiko Maruyama,[5] Yasuyuki Morishita,[6] Etsuko Nakagami-Yamaguchi,[2] Keiki Kumano,[2,7] Hideo Yagita,[8] Masashi Fukayama,[9] Seishi Ogawa,[9,10] Mineo Kurokawa,[7] Koji Yasutomo,[3] and Shigeru Chiba[1,2]

[1]Department of Clinical and Experimental Hematology, University of Tsukuba, Tsukuba, Japan; [2]Department of Cell Therapy and Transplantation Medicine, University of Tokyo Hospital, Tokyo, Japan; [3]Department of Immunology and Parasitology, Institute of Health Biosciences, The University of Tokushima Graduate School, Tokushima, Japan; [4]Laboratory of Cell Therapy, Department of Regenerative Medicine, Clinical Research Center, National Hospital Organization Nagoya Medical Center, Nagoya, Japan; [5]Parasitic Diseases Unit, Department of Infectious Diseases, Faculty of Medicine, University of Miyazaki, Miyazaki, Japan; [6]Department of Pathology, University of Tokyo, Tokyo, Japan; [7]Department of Hematology and Oncology, University of Tokyo, Tokyo, Japan; [8]Department of Immunology, Juntendo University School of Medicine, Tokyo, Japan; [9]Cancer Genomics Project, Graduate School of Medicine, University of Tokyo, Tokyo, Japan; and [10]Core Research for Evolutional Science and Technology, Japan Science and Technology Agency, Tokyo, Japan

Notch receptor-mediated signaling is involved in the developmental process and functional modulation of lymphocytes, as well as in mast cell differentiation. Here, we investigated whether Notch signaling is required for antipathogen host defense regulated by mast cells. Mast cells were rarely found in the small intestine of wild-type C57BL/6 mice but accumulated abnormally in the lamina propria of the small-intestinal mucosa of the *Notch2*-conditional knockout mice in naive status. When transplanted into mast cell–deficient W^{sh}/W^{sh} mice, *Notch2*-null bone marrow-derived mast cells were rarely found within the epithelial layer but abnormally localized to the lamina propria, whereas control bone marrow-derived mast cells were mainly found within the epithelial layer. After the infection of *Notch2* knockout and control mice with L3 larvae of *Strongyloides venezuelensis*, the abundant number of mast cells was rapidly mobilized to the epithelial layer in the control mice. In contrast, mast cells were massively accumulated in the lamina propria of the small intestinal mucosa in *Notch2*-conditional knockout mice, accompanied by impaired eradication of *Strongyloides venezuelensis*. These findings indicate that cell-autonomous Notch2 signaling in mast cells is required for proper localization of intestinal mast cells and further imply a critical role of Notch signaling in the host-pathogen interface in the small intestine. (*Blood*. 2011;117(1):128-134)

Introduction

Mast cells are important in a wide variety of physiologic and pathologic processes, including protective immune responses to parasites and allergic disorders.[1,2] In intestinal parasite infection, mast cells play a central role in the immune response.[3] During the induction phase of parasite-induced inflammation, mast cells move from the submucosa to the tip of the villi, accompanying the serial changes in the protease expression pattern. Initially, they are positive for mouse mast cell protease-5 (mMCP-5) but negative for mMCP-1 and mMCP-2; eventually, they become positive for mMCP-1 and mMCP-2 but negative for mMCP-5, demonstrating convergence from connective tissue–type mast cells (CTMCs) to mature mucosal-type mast cells (MTMCs).[4] The parasite-infected mice consequently experience jejunal mast cell hyperplasia,[5] and the serum concentration of mMCP-1, an activation marker of small intestinal mast cells, is increased by > 1000-fold compared with that in the naive status.[5]

In the mammalian immune system, we and other groups have demonstrated that Notch signaling is involved in the commitment and differentiation of T cells, the development of splenic marginal zone B cells, and the differentiation and functional modulation of mature T cells, including T-helper type I (Th1)/Th2 polarization[6,7] and differentiation of CD8-positive cytotoxic T cells.[8] Regarding the Notch signaling in mast cells, bone marrow-derived mast cells (BMMCs) highly express Jagged1[9] and Notch2[10] among the Notch ligands and the receptors, respectively. We have previously shown that signaling through the Notch2 receptor induces mast cell development from myeloid progenitors by transcriptional up-regulation of hairy and enhancer of split homolog-1 (Hes-1) and transacting T cell–specific transcription factor GATA-3 (GATA3).[11] Induction of antigen-presenting potential of mast cells by Notch signaling is also demonstrated.[12] A question yet to be solved is how Notch signaling affects mast cell properties in vivo.

In this report, we examined the effect of Notch2 signaling in in vivo mast cells using *Notch2*-conditional knockout mice.[13] We show that Notch2 signaling is specifically required for intraepithelial localization of intestinal mast cells and antiparasite immunity. In contrast, Notch2 is dispensable for either distribution or development of CTMCs.

Submitted July 9, 2010; accepted September 28, 2010. Prepublished online as *Blood* First Edition paper, October 22, 2010; DOI 10.1182/blood-2010-07-289611.

The online version of this article contains a data supplement.

The publication costs of this article were defrayed in part by page charge payment. Therefore, and solely to indicate this fact, this article is hereby marked "advertisement" in accordance with 18 USC section 1734.

Methods

Mice

The generation of *Notch2*$^{flox/flox}$ mice was described previously.[13] Mx-*Cre* transgenic mice[14] were crossed with *Notch2*$^{flox/flox}$ mice (*N2*-MxcKO mice) and the progeny were injected with polyinosinic-polycytidylic acid (pIpC; Sigma-Aldrich) 7 times every other day from 3 days after birth (25 μg/g body weight) or 3 times between 4 and 6 weeks of age (20 μg/g body weight). *N2*-MxcKO mice were further crossed with C57BL/6-Ly5.1 mice (a kind gift from Dr H. Nakauchi, University of Tokyo) to generate Ly5.1-*N2*-MxcKO mice. *Notch2* deletion in bone marrow was examined by polymerase chain reaction and 3% agarose gel electrophoresis[13] (supplemental Figure 1, available on the *Blood* Web site; see the Supplemental Materials link at the top of the online article). *W*^{sh}/*W*^{sh} mice were purchased from The Jackson Laboratory. All experiments were done with approval from the University of Tsukuba Institutional Review Board.

Staining

Sections, fixed with Carnoid fluid, were stained with 0.5% toluidine blue (Sigma-Aldrich), pH 0.3, followed by eosin. Small intestine was embedded in optimal cutting temperature (OCT) compound (TissueTek) and cut with cryostat (Leica CM1850). The section was fixed with 4% paraformaldehyde, washed with phosphate-buffered saline (PBS), blocked in 10% horse serum and 0.1% Triton-PBS, and then stained with either 1:100 goat anti-Jagged1 antibody (C-20; Santa Cruz Biotechnology), goat anti-Delta1 antibody (Genzyme Tech), or control goat immunoglobulin G (IgG; Santa Cruz Biotechnology) overnight at 4°C. The sections were washed with PBS and stained with anti–goat Alexa 594 (Invitrogen). Sections were analyzed by fluorescence microscope (Zeiss; Axioplan2), original magnification ×200.

BMMCs

Bone marrow cells from each mouse strain were cultured in RPMI 1640 medium (Sigma-Aldrich) supplemented with 10% fetal bovine serum (FBS), 50 ng/mL stem cell factor (SCF; PeproTech), and 10 ng/mL interleukin-3 (IL-3; PeproTech) for 4 weeks. Generation of BMMCs was confirmed by staining with lineage markers, c-Kit and IgE, as previously described.[11] Briefly, the cells were incubated with purified IgE (BD Biosciences) after blocking the Fcγ receptors with purified anti-CD16/32 antibody (BD Biosciences), stained with anti-IgE–fluorescein isothiocyanate (FITC; BD Biosciences), anti–Gr-1–phycoerythrin (PE), anti-Mac1–PE (eBioscience), and anti–c-Kit–allophycocyanin (APC; eBioscience), and then analyzed by FACSCalibur (BD Biosciences).

Peritoneal mast cells

Five milliliters ice-cold PBS was injected into the peritoneal cavity, and then 3 mL PBS was recovered. c-Kit and IgE receptor (FcεRI) expression was used to define the cells as peritoneal mast cells. Ly5.1 and Notch2 were stained with anti-Ly5.1–PE (BD Biosciences) or biotinylated anti-Notch2 antibody (clone HMN2-35)[8] followed by streptavidin PE (eBioscience), respectively.

Bone marrow transplantation

C57BL/6 mice and *W*^{sh}/*W*^{sh} mice were lethally irradiated with a total dose of 9.5 Gy and then transplanted with 1×10^7 whole bone marrow cells from either *N2*-MxcKO-Ly5.1 mice or *Notch2*$^{flox/flox}$-Ly5.1 mice from the tail vein. Tissues of transplanted mice were assessed at 3 to 4 months after transplantation. Donor-cell engraftment was assessed by fluorescence-activated cell sorting (FACS) analysis of peripheral blood, which was stained by anti-Ly5.2–FITC (BD Biosciences) and anti-Ly5.1–PE.

S venezuelensis infection

Mice were infected by subcutaneous injection of third-stage infective larvae of *Strongyloides venezuelensis*. The degree of infection was monitored by counting the number of eggs per gram of feces. Mast cells were counted and presented as the number per 10 villus crypt units. BMMCs were washed with PBS twice and then cultured with 10 ng/mL IL-4 and 10 ng/mL IL-10 for 3 days. These Th2-conditioned BMMCs were injected at day 3 and day 6 of experiments.[15] In contrast to the bone marrow transplantation, mice were not irradiated before BMMC injection.

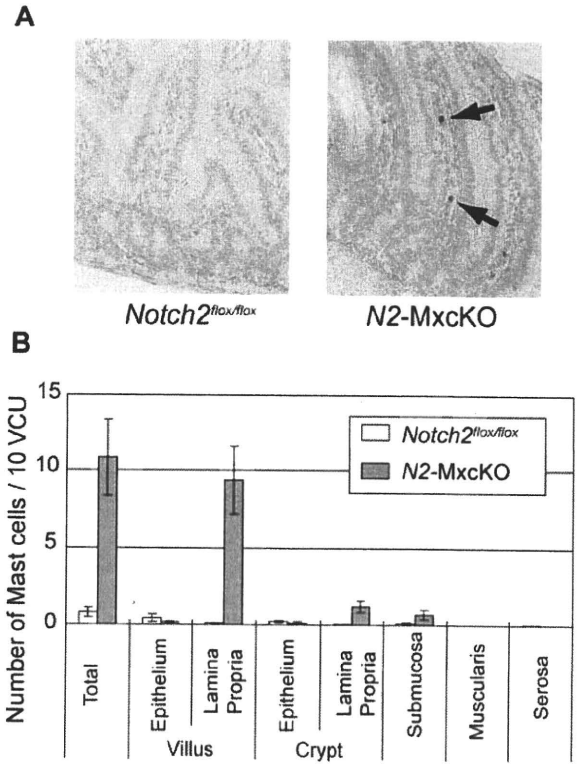

Figure 1. Mature mast cells were abnormally accumulated in the lamina propria of the small intestine of *Notch2*-deficient mice. (A) Sections of the small intestine of *N2*-MxcKO or littermate control *Notch2*$^{flox/flox}$ mice. Toluidine blue staining, followed by eosin. Original magnification ×200. (B) The numbers of mast cells per 10 villus crypt units (vcus) distributing to various layers of the small intestine. Data are presented as means ± SEM; *Notch2*$^{flox/flox}$ (n = 10) versus *N2*-MxcKO (n = 8); $P = .000461$ (total), $P = .000261$ (villus, lamina propria), $P = .001918$ (crypt, lamina propria), $P = .046874$ (submucosa).

Statistical analysis

The data for the number of mast cells and the *S venezuelensis* infection data were analyzed by the *t* test. *P* values < .05 were considered significant.

Results

Notch signaling affects the number and localization of mast cells in the small intestine

We have previously reported that Notch2 regulates mast cell differentiation in vitro.[11] To examine whether Notch2 controls the differentiation or development of MTMCs in vivo, we examined intestinal mast cells by toluidine blue staining in C57BL/6 mice carrying the *Notch2*$^{flox/flox}$ allele with or without the Mx1-*Cre* transgene (*N2*-MxcKO mice or *Notch2*$^{flox/flox}$ mice, respectively) after pIpC treatment.[13] Mast cells were only sparsely detected in the small intestine of *Notch2*$^{flox/flox}$ mice, mainly within the epithelium. However, the total number of mast cells in the small intestine of *N2*-MxcKO mice was unanticipatedly greater than that of *Notch2*$^{flox/flox}$ mice. Furthermore, those mast cells were mainly

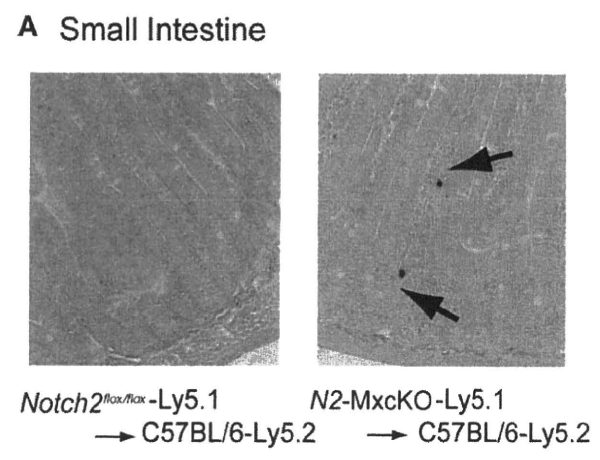

Figure 2. Localization of intestinal mast cells is abnormal in wild-type mice transplanted with *N2*-MxcKO-Ly5.1 bone marrow cells, reminiscent of that in *N2*-MxcKO mice. (A) Bone marrow cells from either *N2*-MxcKO- Ly5.1 mice or littermate *Notch2*$^{flox/flox}$- Ly5.1 mice were transplanted into lethally irradiated (9.5 Gy) C57BL/6-Ly5.2 mice. Toluidine blue staining, followed by eosin. Original magnification ×200. (B) The numbers of mast cells per 10 vcus distributing to various layers of the small intestine. Data are presented as means ± SEM; Mast cells in C57BL/6-Ly5.2 mice transplanted with *Notch2*$^{flox/flox}$-Ly5.1 (n = 3) versus *N2*-MxcKO-Ly5.1 (n = 3). $P = .020594$ (total) and $P = .030123$ (villus, lamina propria).

localized to the lamina propria, and very few mast cells were found within the epithelium (Figure 1A-B).

Localization of MTMCs is abnormal in wild-type mice transplanted with *N2*-MxcKO bone marrow cells, reminiscent of that in *N2*-MxcKO mice

Because the Mx-*Cre*–based conditional knockout system deletes target genes not only in the bone marrow cells but also, albeit partially, in the intestinal cells,[14] there was a possibility that *Notch2* deletion in the intestinal cells was responsible for the distinct distribution pattern or increased number of mast cells in *N2*-MxcKO mice compared with control mice. To exclude this possibility, we transplanted *Notch2*-null bone marrow cells carrying the Ly5.1 marker to irradiated wild-type C57BL/6-Ly5.2 mice. A chimerism of donor-derived Ly5.1-positive fraction accounted for more than 70% in the peripheral blood (data not shown). The recipients of bone marrow cells from *Notch2*$^{flox/flox}$ mice showed that the intestinal mast cell distribution was virtually the same as that in wild-type mice, whereas the recipients of *Notch2*-null bone marrow cells showed an increase in mast cells mainly in the lamina propria in an indistinguishable manner from the *N2*-MxcKO mice (Figure 2A-B). This result indicates that deletion of *Notch2* in bone marrow-derived cells alters the distribution pattern and increases the number of mast cells in the small intestine.

Notch-ligand expression in the small intestine

Notch signaling is known to be activated through Notch ligand-receptor binding.[16] We examined the expression pattern of Notch ligands in the small intestine with antibodies against Notch ligands Jagged1 and Delta1 and found that the epithelial layer was clearly stained with anti-Jagged1 but not with anti-Delta1 antibody (Figure 3). The staining with the anti-Jagged1 antibody was confined to the surface of epithelial cells, especially at their basal side rather than the apical side (Figure 3). The Jagged1 expression pattern suggests a possibility that Jagged1-Notch2 interaction between the basal side of the epithelial cells and mast cells has an important role for mast cell migration from the lamina propria across the basement membrane toward the epithelium (Figure 3). Furthermore, the ligand-receptor binding itself might contribute to mast cell–epithelial cell adhesion to some extent, based on our observation that *Notch2*-expressing BMMCs attached to the Jagged1-expressing Chinese hamster ovary (CHO) cells, while *Notch2*-null BMMCs did not (supplemental Figure 2).

Notch2 is dispensable for the CTMC development and distribution

We next investigated the roles of Notch2 in the development of CTMCs. The localization and the number of CTMCs in the skin and peritoneal cavity were not significantly different between *N2*-MxcKO and littermate *Notch2*$^{flox/flox}$ mice more than 4 weeks after the treatment with pIpC (data not shown). This observation might simply indicate that the Mx-*Cre* system was inefficient in the tissue-resident mast cells, as a great majority of peritoneal

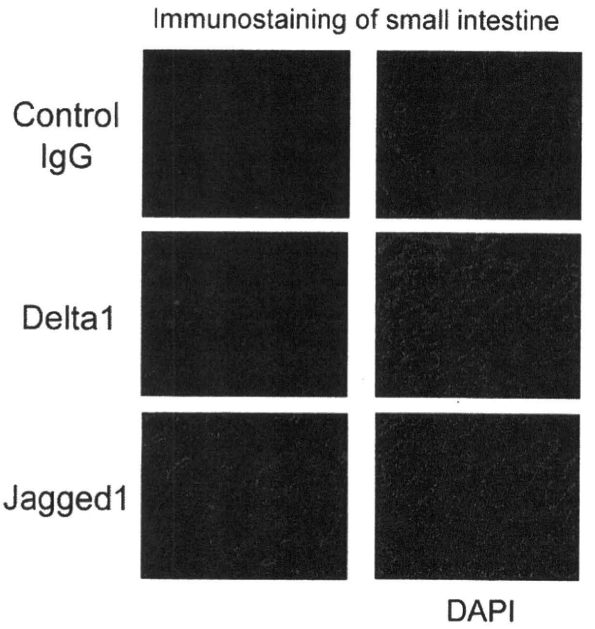

Figure 3. Jagged1 is strongly expressed on the surface of the epithelial cells, especially at their basal side. A section of small intestine prepared using cryostat was stained with goat anti-Jagged1 and goat anti-Delta1 antibodies followed by anti–goat Alexa594. Original magnification ×200.

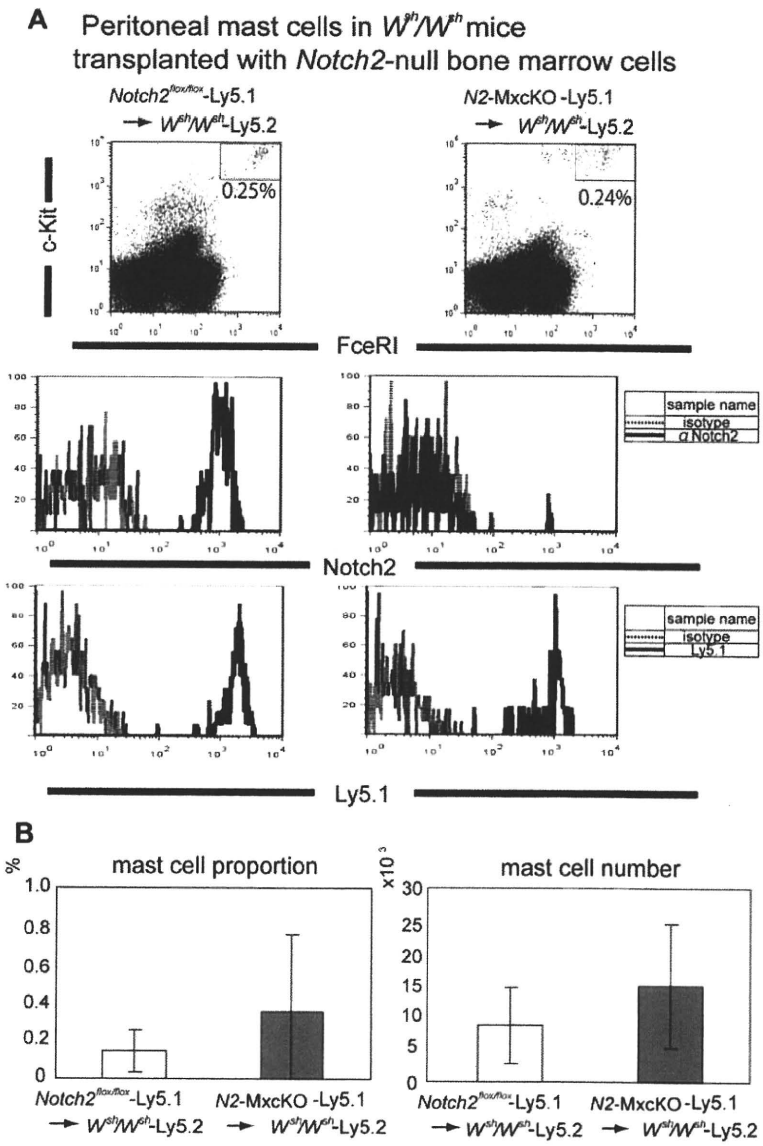

Figure 4. Notch2 is not required for peritoneal mast cell development. (A) Bone marrow cells from *N2*-MxcKO-Ly5.1 mice or control *Notch2*$^{flox/flox}$-Ly5.1 mice were transplanted into lethally irradiated *W*^{sh}/*W*^{sh} mice. Peritoneal mast cells were stained with anti–c-Kit–APC, IgE, and biotinylated anti-Notch2 antibody (HMN2-35), followed by anti-IgE–FITC and streptavidin-PE, or they were stained with anti–c-Kit–APC, IgE, and anti-Ly 5.1–PE, followed by anti-IgE–FITC; they were then analyzed by FACSCalibur (BD Biosciences). (B) The proportion (left) and the absolute number (right) of peritoneal mast cells were not significantly different between *W*^{sh}/*W*^{sh} mice transplanted with *Notch2*-WT bone marrow cells and those transplanted with *Notch2*-null bone marrow cells. $P = .210642$ (mast cell proportion) and $P = .196045$ (mast cell number).

mast cells of pIpC-treated *N2*-MxcKO mice still expressed Notch2 (data not shown). Therefore, to clarify the requirement of *Notch2* in the CTMC development, we examined peritoneal mast cells in mast cell-deficient *W*^{sh}/*W*^{sh} mice after transplantion of *Notch2*-null bone marrow cells carrying the Ly5.1 marker. In this system, mast cells exclusively develop from transplanted bone marrow progenitors, in which the *Cre* recombinase under the Mx-promoter is quite effective [14] (supplemental Figure 1). In this experiment, we found that the proportion and absolute number of peritoneal mast cells was not significantly different between those developed from the *N2*-MxcKO-Ly5.1 bone marrow cells and those developed from littermate *Notch2*$^{flox/flox}$-Ly5.1 bone marrow cells (Figure 4A-B). Notch2 was not expressed in the peritoneal mast cells derived from *N2*-MxcKO-Ly5.1 bone marrow cells but was expressed in those derived from littermate *Notch2*$^{flox/flox}$-Ly5.1 bone marrow cells (Figure 4A middle), indicating that *Notch2* was deleted efficiently. These results suggest that Notch2 is dispensable for the development and distribution of CTMCs.

Cell-autonomous Notch2 signaling in mast cells is important for mast cell migration across the basement membrane in the small intestine

We then asked a question whether aberrant mast cell migration in the small intestine in *N2*-MxcKO mice is dependent on Notch2 signaling in mast cells per se. We intravenously infused *Notch2*-null or control BMMCs into nonirradiated *W*^{sh}/*W*^{sh} mice after *S venezuelensis* infection, because it is reported that BMMCs could only transiently reconstitute intestinal mast cells in mast-cell deficient mice if these recipient mice are in naive status.[17] In tissue sections, we found that the distribution of mast cells in the small intestine was different between control BMMCs-reconstituted mice and *Notch2*-null BMMCs-reconstituted mice; control BMMCs were mainly migrated into the epithelial layer, while a majority of *Notch2*-null BMMCs remained in the lamina propria. This observation indicates that mast cell-autonomous Notch2 expression contributes to mast cell migration across the basement membrane from lamina propria into the epithelial layer (Figure 5A-B). Even in the control BMMC-infused mice, however, a substantial proportion of

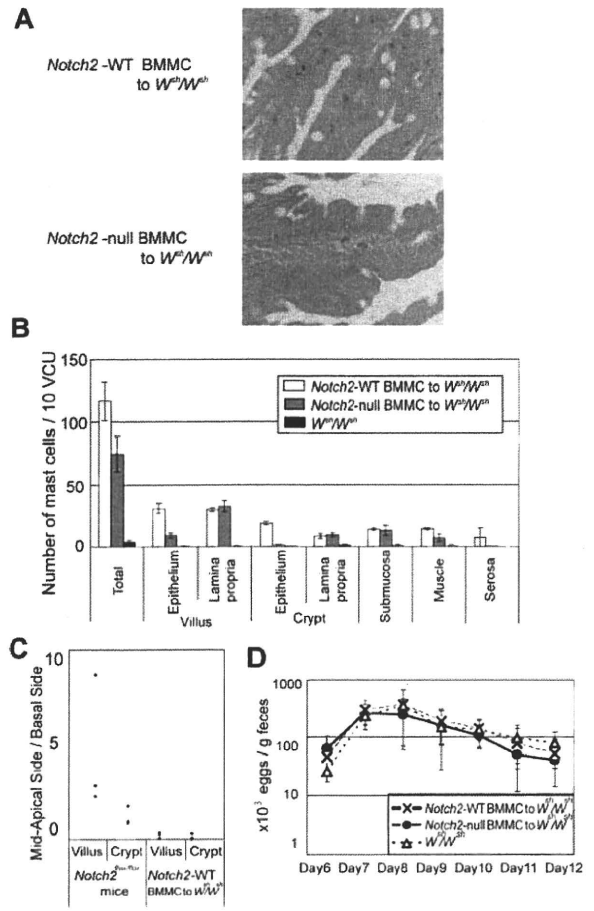

Figure 5. Mast cell–autonomous Notch2 expression is required for mast cell migration toward the epithelium. W^{sh}/W^{sh} mice infected with *S venezuelensis* were intravenously infused with Th2-conditioned *Notch2*-null or control BMMCs on days 3 and 6 of infection. (A) *Notch2*-null BMMCs poorly migrated toward the epithelium compared with control BMMCs. Toluidine blue staining followed by eosin staining. Original magnification ×200. (Top) Control BMMCs; (Bottom) *Notch2*-null BMMCs. (B) The number of mast cells per 10 vcus in the small intestine on day 12 after *S venezuelensis* infection in W^{sh}/W^{sh} mice, without BMMC infusion, with control BMMC infusion, and with *Notch2*-null BMMC infusion. Data are presented as means ± SEM; n = 3 (control BMMC infusion) and n = 4 (*Notch2*-null BMMC infusion), $P = .004080$ (villus, epithelium) and $P = .000020$ (crypt, epithelium). Note that mast cells in W^{sh}/W^{sh} mice infused with *Notch2*-null BMMCs abnormally resided in the lamina propria, whereas most of those in W^{sh}/W^{sh} mice infused with control BMMCs had intraepithelially migrated. (C) Mast cell number in mid to apical side of the epithelial layer was divided with that in the basal side of the epithelial layer. (D) Time course of *S venezuelensis* egg numbers in the stool. The number of excreted eggs was not significantly different between W^{sh}/W^{sh} mice infused with *Notch2*-null and control BMMCs. Data are presented as means ± SEM.

mast cells still remained in the lamina propria, submucosa, and smooth muscle layers, and the distribution of mast cells within the epithelium was confined to the basement membrane side of the epithelial layer (Figure 5B-C). This mast cell localization pattern was different from that in the $Notch2^{flox/flox}$ mice with *S venezuelensis* infection, in which mast cells were present mainly at the mid to apical side of the epithelial layer (Figure 5C). The numbers of *S venezuelensis* eggs in the stool were virtually the same in the *S venezuelensis*–infected W^{sh}/W^{sh} mice infused with *Notch2*-null and control BMMCs and in the *S venezuelensis*–infected W^{sh}/W^{sh} mice without any BMMC infusion throughout the period after infection (Figure 5D).

Taken together, the BMMC-W^{sh}/W^{sh} transplantation model demonstrated that Notch2 in the mast cells indeed determines their intraepithelial migration from lamina propria; nevertheless, this model was not adequate to examine the physiologic mast cell distribution pattern and subsequent parasite expulsion that depends on mast cells.

Notch2 signaling regulates antiparasite immunity of mast cells in the intestine

The BMMC-W^{sh}/W^{sh} reconstitution model could not completely reflect physiologic mast cell distribution pattern in the small intestine. Therefore, to further assess the effect of Notch2 signaling on the mucosal immune response of intestinal mast cells under a pathologic condition, *N2*-MxcKO or control $Notch2^{flox/flox}$ mice were infected with *S venezuelensis*. Total mast cell number was increased in $Notch2^{flox/flox}$ mice much more than in *N2*-MxcKO mice, especially in the epithelium in both crypts and villi 8 days after infection (Figure 6A-B). Thirteen days after infection, mast cells in the epithelium in $Notch2^{flox/flox}$ mice were still more abundant than those in *N2*-MxcKO mice (Figure 6C-D), while mast cell accumulation in the lamina propria in *N2*-MxcKO mice was more prominent in both villi and crypt than that in the earlier stage of infection (Figure 6A,C). In particular, dense aggregation of mast cells was prominent in the lamina propria of *N2*-MxcKO mice at the tip of the villi (Figure 6D). As a consequence, the total number of mast cells in the intestine of *N2*-MxcKO mice became equivalent to those of $Notch2^{flox/flox}$ mice 13 days after infection (Figure 6C,E). The number of *S venezuelensis* eggs in the stool was gradually decreased during day 8 to 10 in control $Notch2^{flox/flox}$ mice but not in *N2*-MxcKO mice (Figure 6F). Furthermore, the worms were still observed in *N2*-MxcKO mice but not in $Notch2^{flox/flox}$ mice 12 days after infection (Figure 6G). These data suggest that Notch2 deficiency alters the distinct distribution pattern of mast cells in the small intestine, which is responsible for the defective eradication of *S venezuelensis*.

Discussion

There is a growing body of evidence that Notch signaling modulates cellular migration and adhesion in endothelial, neural, and lymphoid lineage cells, as well as cancer cells.[18] We have shown that Notch2 signaling induces the development of mast cells.[11] However, it has remained unclear whether Notch2 signaling is involved in the distribution of mast cells in the intestinal mucosa or connective tissues or in controlling the functions of mast cells against microorganisms. Here, we investigated the role of Notch2 signaling in mast cells in terms of their distribution and functions using cell-specific *Notch2*-deficient mice. We found that in *N2*-MxcKO mice, mast cells were abnormally accumulated in the lamina propria of the small intestine, suggesting that *Notch2*-null mast cells have some defect in the migration toward the epithelium. Furthermore, *N2*-MxcKO mice failed to eradicate *S venezuelensis* and exhibited a distinct mast cell migration pattern in the intestine compared with control mice, suggesting that mast cells regulate the host-microbial interface in the intestine through Notch2 signaling.

Mast cell number was rather increased in the intestinal mucosa of *N2*-MxcKO mice compared with control mice in naive status. Mast cell progenitors were supposed to reside in the submucosa and gradually move toward the villi, accompanied by their differentiation into mature mast cells. Based on our observation in